GEST-2062

FINAL TECHNICAL SUMMARY REPORT OF RESEARCH AND DEVELOPMENT PROGRAM OF THERMIONIC CONVERSION OF HEAT TO ELECTRICITY

Volume I

July 1968

Contract Number NObs-90496
Project Serial Number SR-007-12-01
Order Number ARPA 219, Task No. 1 and No. 2
Program Code Number 3980

General Electric Company
NUCLEAR THERMIONIC POWER OPERATION
P. O. Box 846
Pleasanton, California

GEST-2062

FINAL
TECHNICAL SUMMARY REPORT
OF
RESEARCH AND DEVELOPMENT PROGRAM
OF
THERMIONIC CONVERSION OF HEAT TO ELECTRICITY

Volume I

July 1968

This work was supported by ARPA funds
through United States Navy, Bureau of Ships
Contract Number NObs-90496

Project Serial Number SR-007-12-01
Order Number ARPA 219, Task No. 1 and Task No. 2
Program Code Number 3980

General Electric Company
NUCLEAR THERMIONIC POWER OPERATION
P.O. Box 846
Pleasanton, California

LEGAL NOTICE

TABLE OF CONTENTS

LIST OF ILLUSTRATIONS

LIST OF ILLUSTRATIONS
(Continued)

LIST OF TABLES

I. INTRODUCTION

This is Volume I of the second semi-annual and final technical summary report describing progress of the research and development program on thermionic conversion of heat to electricity under the Department of the Navy, Bureau of Ships Contract NObs-90496. The work performed under this contract is based upon and is a continuation of work initiated under contract NObs-88578. Both contracts were issued by the U. S. Navy, Bureau of Ships, and supported by the Advanced Research Projects Agency.

The objective of this program is the development of a nuclear thermionic electrical generating system for the Department of the Navy. Work under this contract is being performed to develop the material capabilities which are essential for this nuclear thermionic system. This work consists of three major tasks. They are:

TASK A - UO_2 - Refractory Metal Reaction Kinetics

This task includes:

(1) A continuation of a series of 1000 hour diffusion experiments of UO_2-molybdenum and UO_2-tungsten fuel-emitter pairs in the temperature regime of 1600 to 1800°C for molybdenum and 1800 to 2200°C for tungsten. The purpose of this effort is the quantitative identification of uranium diffusion (if any) through the refractory metal and the limits of the

uranium diffusion rates. This will be accomplished by alpha particle counting techniques. Metallographic and electron microprobe analysis will be employed to document the extent and nature of solid state reactions.

(2) The determination of the diffusion rate of transport of oxygen through molybdenum or tungsten in the temperature range of 1500 to 1800°C. Thin walled tubes of refractory metals will be heated electrically in a cover gas of flowing purified argon. Known particle pressures of oxygen will be introduced inside the metal tubes and the argon steam monitored for oxygen content.

TASK B - Insulator Materials Development

This task includes the identification of the gaseous species and products which exist when high purity alumina bodies and niobium and/or niobium-1% zirconium are heated to temperatures of interest to elucidate possible gas-solid reactions in a thermionic converter.

TASK C - Ceramic-to-Metal Seal Development

This task includes:

(1) The development of cesium-resistant metallizing coatings for pure alumina ceramics.

(2) The development of molybdenum-alumina cermet structures for use as emitter-collector seal insulators.

(3) The evaluation and/or development of methods of bonding the metallic surface of insulators to structural metal members.

(4) Long-time testing of materials and seals at high temperatures in both vacuum and cesium vapor environments.

The work accomplished under Tasks A and B is included in this volume. Task C is reported in Volume II.

The over-all project responsibility for contract NObs-90496 at the General Electric Company is held by Dr. John E. VanHoomissen, Manager, Nuclear Thermionic Power Operation. The technical contributors with primary responsibility for the individual tasks are:

TASK A-1 - A. I. Kaznoff, Nucleonics Laboratory

TASK A-2 - R. A. Ekvall, A. I. Kaznoff, L. N. Grossman, Nucleonics Laboratory

TASK B - L. N. Grossman and A. I. Kaznoff, Nucleonics Laboratory

TASK C - R. H. Bristow, Tube Department

II. SUMMARY

The work performed under contract NObs-90496 is described in detail in Sections III of this volume and Volume II. Volume II also presents in Section II a summary of the work accomplished in Task C. Tasks A and B are summarized below.

TASK A - UO_2 - Refractory Metal Reaction Kinetics

Sub-task A-1 - UO_2 Diffusion Studies

The diffusion rates of uranium through tungsten when the tungsten is used to encapsulate urania was determined in the temperature range between 1800 and 2000°C. Similarly the diffusion rates of uranium through molybdenum when the molybdenum is used to encapsulate urania was determined in the temperature range between 1600 and 1750°C. The tests were performed with vapor deposited tungsten and slightly hyperstoichiometric urania and with several types of molybdenum using both hyper-and hypostoichiometric urania. The measured diffusion rates with the urania-tungsten were 6.33×10^{-9} gm/hr cm^2 at 1800°C and $< 2 \times 10^{-10}$ gm/hr cm^2 at 2000°C. With urania-molybdenum the rates ranged from 1.1×10^{-10} gm/hr cm^2 at 1600°C to 4×10^{-6} gm/hr cm^2 at 1750°C and the rates varied with the type of molybdenum and the stoichiometry of the urania. It was generally concluded that the steady state diffusion rates are of such magnitude that uranium diffusion through both tungsten and molybdenum is not likely to affect their performance as thermionic emitters

Sub-task A-2 - Oxygen Diffusion Studies

The activation energy and diffusivities for the diffusion of oxygen through polycrystalline molybdenum were determined in the temperature range 1500 to 1800°C. The two experimental techniques used to measure the diffusivities yielded comparable results. The activation energy and diffusivities were based, in part, on interpolation of existing data on the solubility limit of oxygen in molybdenum. The activation of energy was 67.2 ± 20% Kcal/mole and the diffusivities ranged from 5×10^{-8} cm^2/sec at 1500°C to 7.8×10^{-7} cm^2/sec at 1800°C. The diffusivities are known to within +50%.

TASK B - Insulator Materials Development

A mass spectrometric and thermogravimetric study of the equilibrium interaction between alumina and niobium between 1500 and 1900°C has been conducted. The reaction proceeds principally as $Al_2O_3 + 3Nb = 2Al(g) + 3NbO(s)$; a secondary reaction of almost equal importance under neutral conditions is $Al_2O_3 + Nb + 1/2\ O_2 = Al_2O(g) + NbO_2(g) + NbO(s)$. The latter reaction can dominate under oxidizing conditions. The weight loss due to the gaseous reaction products is about one hundred times the weight loss due to evaportaion of alumina under neutral conditions. Calculations show that some heavier stable oxides (e.g., yttrium oxide and thorium oxide will not interact signifi-

cantly with niobium. Gaseous reaction products over beryllia-niobium are comparable to the decomposition pressure of beryllia.

III. TECHNICAL PROGRESS

TASK A - UO_2 - Refractory Metal Reaction Kinetics

Sub-Task A-1 - UO_2 Diffusion Studies

Introduction

The incorporation of thermionic converters in a nuclear reactor core requires the use of emitter structures containing nuclear fuel. The fuel-cladding composite structure operates at high temperatures (>1500°C). Selection and specification of materials to meet these needs requires the prior determination of compatibility of the fuel with the cladding, the transport rates of fuel material through the cladding, the contamination of the cladding surface by the fuel components, and the effects of thermal cycling. This work was directed to the study of these phenomena, under well-defined conditions, for the urania-tungsten and urania-molybdenum systems. These systems represent some of the most stable and compatible combinations of nuclear fuel and emitter materials. During the last five years the compatibility of these systems was established by exhaustive experimental work.[1,2] The stability of urania with tungsten and molybdenum was shown for periods up to 10,000 hours at thermionic design temperatures.

The specific objective of Sub Task A-1 was to continue prior studies on the diffusion of uranium, from urania, through

tungsten and to initiate studies for molybdenum. The tests for tungsten were to be performed in the range of 1800 - 2200°C and for molybdenum primarily in the range of 1600 - 1700°C. The magnitudes of diffusion fluxes were to be ascertained by alpha-counting techniques; auxiliary analytical techniques were to be employed to verify the findings.

Experimental Techniques & Procedures

The study of interactions of fuel with the cladding material was conducted with encapsulated fuel (Figure 1). The diffusional transport was observed across the 20-mil thick "window" in the capsule. The provision of much thicker walls and end-closure served to limit the diffusion transport in directions other than through the window. Consequently, the capsule system approximated a one-dimensional diffusion experiment. The capsule was heated by electron bombardment on the capsule face opposite the window. This method of heating produced temperature gradients in the capsule and in the fuel. The temperatures were measured by optical pyrometry on the two black-body holes in the thick walls of the capsule. This pyrometry established the temperature at the cladding "window" - fuel interface and the gross temperature gradient. The temperature gradient across the fuel was calculated to be 200°C/inch at 1800°C and 480°C/inch at 2200°C. The test temperatures cited refer always to the

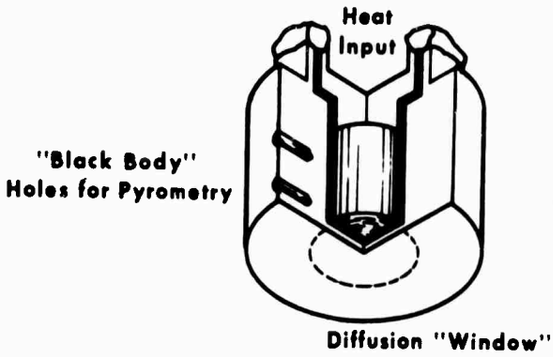

Overall Height	0.340 inch
Base to Shoulder	0.265 inch
Diameter	0.435 inch
Window Thickness	0.020 inch

FIGURE 1. DIFFUSION CAPSULE

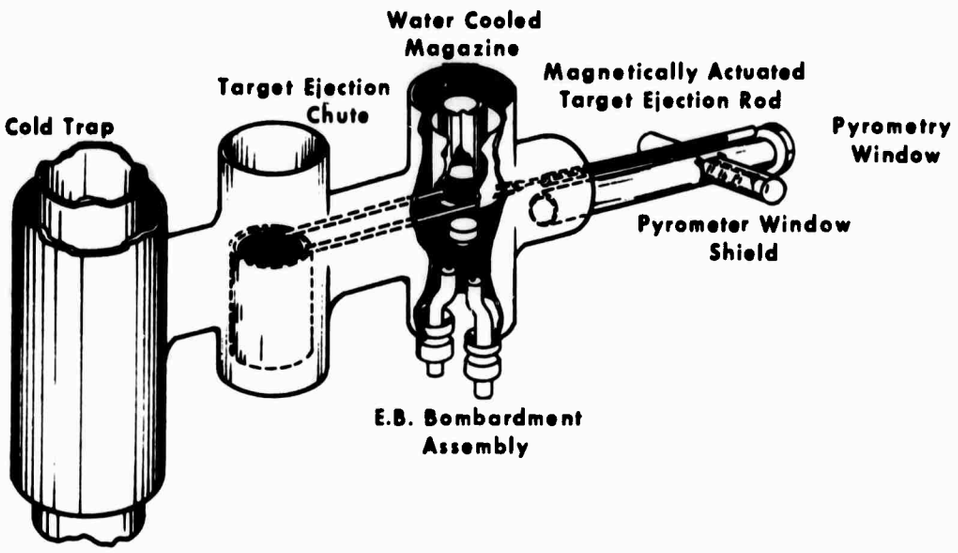

FIGURE 2. DIFFUSION TEST APPARATUS

fuel-cladding interface at the diffusion "window". The presence of temperature gradients simulated, qualitatively, the thermal regime in the reactor where temperature gradients are always present. These temperature gradients are of major importance because they provide the driving force for urania redistribution, i.e., the sublimation of the nuclear fuel and its redeposition at regions of lower temperatures (the cladding). Deposition on the cladding provides and ensures intimate contact between fuel and cladding and substantially lowers the thermal impedance of the fuel-cladding interface. Temperature gradients can also account for the sublimation fractionation of the more volatile phases formed in the fuel body as a result of stoichiometry changes or fission product buildup.

The tests were made in vacuum between 3×10^{-7} and 8×10^{-8} torr. The diffusing species through the 20-mil cladding thickness were free to volatilize from the outer surface. The condensibles of the diffusing flux were trapped on cold (20°C) aluminum targets which were placed directly opposite the "window" area in a water-cooled magazine. The basic components of the test device are shown in Figure 2. Periodically, the targets were removed through a vacuum interlock without interrupting the test and analyzed for uranium content. The capability of sampling without interrupting the test conditions

was a very desirable feature. Apart from increasing the utilization of the device by this sampling technique, it was also noted that shutdowns (cooldowns and heatups) could affect the results.

The fuel used in this work was fully enriched urania. This selection was made as a result of two considerations: (a) To differentiate the uranium obtained as a result of diffusion from the trace residual natural uranium found in refractory metals and (b) To increase the sensitivity of the alpha counting technique by virtue of the high U-234 and U-235 content in enriched urania which is not available in natural urania.

The primary analytical technique, alpha counting, showed that high sensitivity could be achieved. One count per minute represented 1.325×10^{-8} gm of total uranium transport. The counting was sensitive to at least 0.1 count/min. above background. It is believed that a sensitivity to 1.3×10^{-9} gm of uranium was achieved. The main sensitivity was obtained from the U-234 content.

The secondary analytical technique was dilution mass spectrometry in which an internal calibration (spike) of U-233 was used. Generally, the results were obtained on U-235 and U-238 content (where possible U-234 was also determined). The determination of isotopic content was necessary to

eliminate doubts that the uranium activity observed was due to the enriched fuel which was diffused and not due to the residual uranium in the test components. It was found that U-238:U-235 ratios were higher than those in the enriched fuel. This indicated the "boil-out" of the natural uranium impurity in the refractory metals. This contribution was far too small to affect alpha counting techniques, which were dependent primarily on U-234, or the contents of U-235 obtained by mass spectrometry.

The correspondence between mass spectrometry and alpha counting was good, especially for uranium contents about 10^{-9} gm. The typical correspondence obtained on actual test targets was:

	Amount of U-235 (gm)	
Test	Alpha Counting	Mass Spectrometry
1	1.89×10^{-7}	1.75×10^{-7}
2	1.3×10^{-9}	0.54×10^{-9}

Generally, mass spectrometry gave lower results than alpha counting which suggests that the geometric factor in alpha counting was lower than anticipated, or more probably, that there was some uranium loss in the chemical separation steps leading to mass spectrometric determinations.

Mass spectrometric analysis of blank targets showed that U-235 content was less than 10^{-11} gm. Every target was alpha-counted before use to eliminate the possibility of accidental contamination. Repeated checks on target cross-contamination in the experimental apparatus showed negative results. A comparison of alpha-counting and mass spectrometry results indicated that contamination of targets by sublimates of tungsten and molybdenum did not affect the determination of uranium by alpha-counting to any appreciable extent.

Supplementary details on the experimental apparatus and analytical procedures have been reported.[3]

Materials Characterization

The UO_2 chemical analysis was carried out on both powder and sintered product. The sintered pellet product was approximately 95% of theoretical density, and was cut to size by an ultrasonic cutter.

TABLE 1

Characterization of Urania

Chemical Analysis

	UO_2 Powder as-received (ppm)	UO_2 Sintered Pellets (ppm)	Comments
Al	< 5.0	25.0	Increase
B	0.1	0.6	Unchanged
C	100.0	5.0	Large decrease
Cd	< 0.2	< 1.0	Unchanged
Co	1.0	-	
Cr	6.0	20.0	Increase
Ca	0	1.0	Unchanged
F	<50.0	< 5.0	Decrease
Fe	20.0	75.0	Pick-up
Mg	4.0	10.0	Virtually unchanged
Mn	2.0	4.0	Virtually unchanged
Mo	11.0	10.0	Unchanged
Na	1.0	-	
Ni	10.0	50.0	Increase
Pb	< 1.0	< 1.0	
Si	20.0	60.0	Increase
Sn	< 1.0	< 1.0	
V	-	< 15.0	
O/U	2.04	2.0042	Significant decrease
Density	10.25 - 10.5 gm/cc (theoretical 10.97 gm/cc)		

Isotope Analysis	Batch I	Batch II
U-235	93.50 %	92.78 %
U-234	1.065 %	1.25 %
U-238	5.385 %	5.743 %

The tests were conducted on the following cladding materials:

	<u>Tungsten</u>
W-SFVD	San Fernando vapor deposited (hydrogen reduction of WF_6).
	<u>Molybdenum</u>
Mo-PM	General Electric power metallurgy sintered stock.
Mo-AC	General Electric arc cast.
Mo-1/2 Te	General Electric Mo-1/2% Ti.

The typical analyses for these materials are shown on the following page in Table 2.

TABLE 2

Chemical Analyses of Refractory Claddings (in ppm)

Element	W-SFVD	Mo-AC	Mo-PM
C	22-24	100-210	60-160
O	6-60	30	< 20
N	6-20	20	20
Hf		< 100	< 100
Al	< 10	< 50	< 50
Cd		< 100	< 100
Cr	< 10	< 50	< 50
Cu	< 10	< 50	< 50
Fe	< 10	< 50	< 50
Ni		< 50	< 50
Si	< 10	< 50	< 50
Sn	< 10	< 50	< 50
Zr	< 25	< 100	< 100
Cb	< 100	< 100	< 100
Ta	< 250	< 200	< 200
Zn		< 100	< 100
Ca		< 50	< 50
Cb		< 100	< 100
Na		< 100	< 100
Ti	< 10		
Mo	< 10	Major	Major

The largest variations between lots and within lots are in carbon and oxygen content. With the exception of W-SFVD, the materials were obtained in rod form, which was machined into the capsule configuration. Vapor-deposited tungsten was obtained in sections suitable for incorporation as the capsule structure. Closures on capsules were made by TIG welding.

Experimental Results. Urania-Tungsten. The summary of the tests conducted on $UO_{2.0042}$ and tungsten (vapor deposited capsules) are given below.

Test	Tungsten Type	Temperature (^{o}C)	Test Duration (hours)	Average Uranium Flux ($gm/hr\text{-}cm^2$)	No. of Thermal Cycles
1.	W-SFVD	1800	1273	6.33×10^{-9}	1
2.	W-SFVD	2000	1565	$< 2 \times 10^{-10}$	1

Urania-Molybdenum. A summary of test results is given in Table 3. (molybdenum test number is marked with an asterisk to differentiate from the tungsten test in further discussions).

TABLE 3. Urania-Molybdenum Test Results

Test No.	Molybdenum Type	Urania O:U Ratio	Temp (°C)	Test Duration (hours)	Average Uranium Flux ($gm/hr - cm^2$)	No. of Thermal Cycles
1*	AC-1	2.0042	1750 1450	250 380	1.3×10^{-10} Transient with high peak rate	1
2*	AC-1	2.12	1750	48	High initial rate of 4×10^{-6} decreasing rapidly to 10^{-9}	
3*	AC-1	1.91	1750 1605	320	$\sim 6 \times 10^{-9}$ Decreasing to 3×10^{-10}	1
4*	AC-1	2.0042	1600 1700	1100 400	1.1×10^{-10} 1.6×10^{-10}	2
5*	AC-2	2.0042	1750 1600	300 700	4×10^{-6} 10^{-7}	2
6*	PM	2.0042	1600	1500	10^{-7} decreasing to 10^{-8}	3
7*	Mo-1/2 Ti	2.0042	1600	1000	1.2×10^{-10}	

Shown in Figure 3 are the results of Test 4 and Test 1 *. The results of Tests 2 and 3 are shown in Figures 4 and 5.

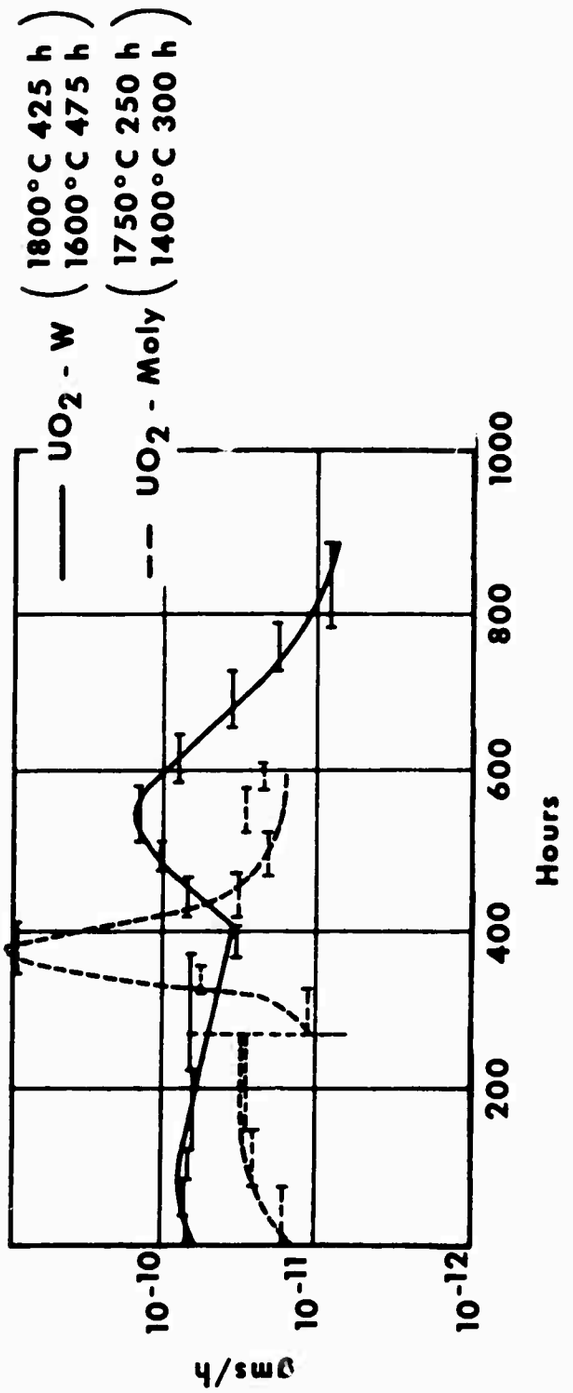

FIGURE 3. DIFFUSION AND CYCLING DATA FOR W-UO_2 AND Mo-UO_2

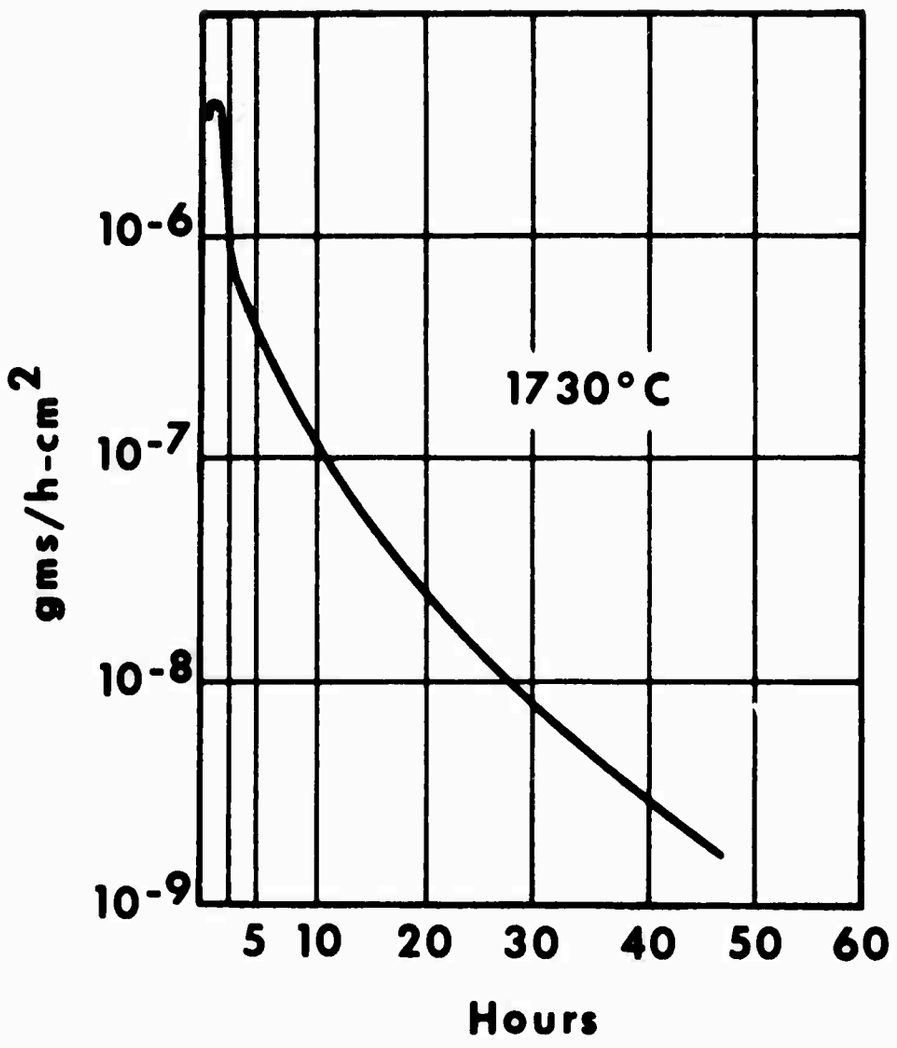

FIGURE 4. #1 MOLY/$UO_{2.1}$ (Bubble formed - 25 minutes)

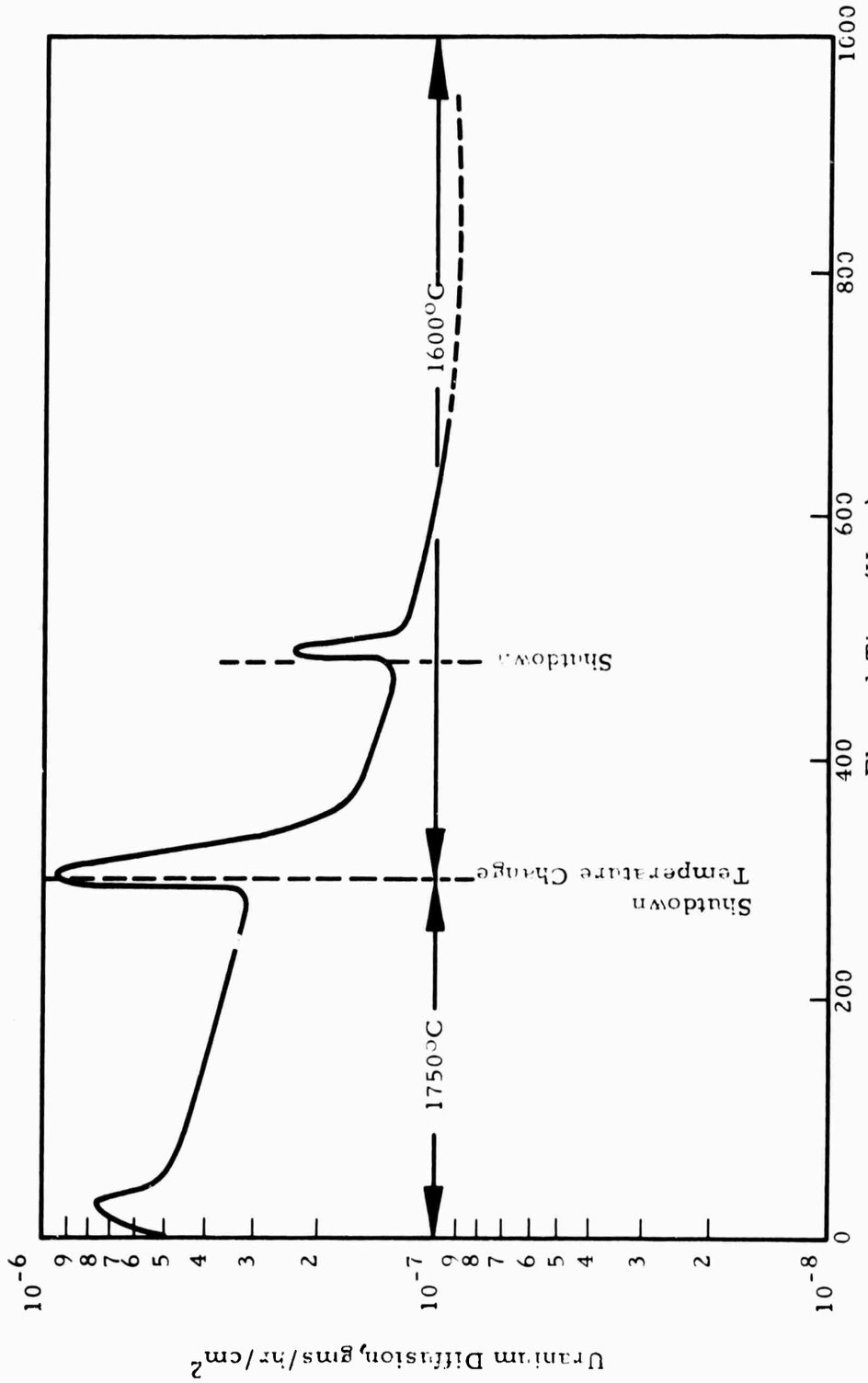

FIGURE 5. DIFFUSION OF URANIUM THROUGH ARC-CAST MOLYBDENUM

Discussion of Results

The results cited for vapor-deposited tungsten (Test No. 1) represents the average flux over the test period. The actual diffusion flux started at a high rate of 8.2×10^{-8} gm/hr cm^2 and leveled out during the last 700 hours to 2.75×10^{-9} gm/hr cm^2. Within the limitations of this experimental program and analytical capability the results show that GE powder metallurgy tungsten, tested in the previous program year, showed the lowest uranium diffusion rate followed by arc-cast tungsten and then followed by the vapor deposited tungsten. However, it should be noted that surface contamination due to absorbed uranium atoms, had been shown to be only about 1/100 of a monolayer for tungsten claddings used. It should be also noted that in all instances the transport rates were very low and remained low at higher temperatures, which are above the temperatures necessary for systems design and application. It is not known why the test at 2000°C produced lower apparent rates than that at the lower temperature of 1800°C. Vapor-deposited tungsten showed very minor grain growth and the columnar grain structure, oriented parallel to the diffusion path, remained virtually unchanged. In this structure there was essentially one grain in the 20-mil cladding. This microstructure may account for the larger diffusion rates when compared to the other types of tungsten. The observed trend is higher diffusion rates for larger grain

sizes. In all cases the grain size in the diffusion "window" area of the capsule was the same as in the rest of the capsule body which indicates that this diffusion cannot be expected to change the microstructure and electron emission.

Cycling seemed to promote the penetration of urania into the grain boundaries to a limited depth of about 1 to 3 mils. Electron microprobe examination was used to identify these uranium-bearing deposits. It is postulated that the mechanism for this penetration is as follows: On cooldown, free uranium metal is produced by the reaction:

$$\frac{2}{2-x} \quad UO_{2-x} \rightarrow UO_2 + \frac{x}{2+x} \quad U.$$

The elemental uranium penetrates the grain boundary. On reheating to the original temperature, the uranium in the grain boundary can reoxidize by the diffusion of oxygen from the UO_2 next to it. The reverse reaction takes place

$$\frac{x}{2-x} \quad U + UO_2 \rightarrow \frac{2}{2-x} \quad UO_{2-x}.$$

This results in a racheting mechanism which can lead to failure. This attack is not general and is not observed at all grain boundaries. This leads one to suspect that only those grain boundaries which happen to be in contact with a uranium precipitate are affected. The kinetics of this process are undoubtedly affected by cooling and heating rates, the diffusion rates of uranium in the cladding, and oxygen dif-

fusion in uranium and urania. At temperatures of interest to thermionics, such attack is very minor. This attack can be expected to increase in severity with higher temperatures and in environments favoring a higher extent of sub-stoichiometry (i.e., reducing conditions) in the urania fuel and power cycling.

The urania fuel was hypostoichiometric after the test in all test capsules; final O:U ratio was of the order of 1.99. The hypostoichiometry increased with increase in temperature as is evident from metallographical examination. Minor amounts of tungsten precipitates were found in the urania fuel. These precipitates were probably formed in the initial heatup period when the oxygen content of the fuel was still high. Pore migration up the temperature gradient in urania was observed in all specimens.

The results of tests in the system Mo-UO_2 showed that diffusion rates at 1600 to 1750°C [6] were comparable to those in the W-UO_2 system at 1800 to 2200°C [5]. The high rates in Tests 5* and 6* may be attributed to the high carbon content in the molybdenum but a definitive explanation is not available at this time. The main result of Test 1* was that it demonstrated that cycling again produced high peak fluxes as was shown in an earlier study (See Figure 3 W-UO_2).

Test 2* was designed to explore the effects of excess oxygen. It was clearly shown that very high diffusion fluxes resulted and decayed rapidly with time (Figure 4). This was not unexpected because of previous studies of the reactions in the Mo + UO_{2+x} system.[7] The main feature of the reaction is the formation of low metling uranium-molybdenum-oxygen compound. This compound attacks and penetrates grain boundaries of molybdenum cladding. In a reducing environment and at high temperatures, this compound is unstable and decomposes by losing oxygen, to yield finally urania and molybdenum. The evidence for this reaction can be readily seen by inclusions of urania in the grain boundaries of molybdenum and molybdenum in the urania body. The effect on the diffusion rate of uranium through molybdenum, under these excess oxygen conditions, is a large increase compared with the results for stoichiometric urania. Loss of oxygen which brings the system closer to stoichiometry reduces the diffusion rate. Internal pressures developed in this capsule were sufficient to distort the structure.

By testing an O:U ratio of 1.91 in Test 3*, it was shown that higher diffusion rates will be observed if the fuel consisted of urania and uranium at the test temperature. This test confirmed the hypothesis advanced for the cycling phenomena observed. As a consequence of these tests, it

can be concluded that no benefits accure from the use of hypo- or hyperstoichiometric urania from the criterion of lowering the diffusion rates.

At present, it is premature to conclude that arc-cast molybdenum is superior to powder metallurgy molybdenum. It is conceivable that control of interstitial impurities may be an important factor, particularly if one considers that impurities such as carbon can produce reducing conditions and may be areas susceptible to attack on the grain boundaries. It was established that in all tests the fuel became hypostoichiometric as in the case of UO_2-W

$$UO_2(s) \rightarrow UO_{2-x}(s) + \frac{x}{2} O_2 \uparrow$$

The oxygen was lost either as elemental oxygen or as metal oxides, by diffusion and volatilization from the capsule. On cooldown (typically at or below 1600°C) the hypo-stoichiometric phase is unstable with respect to urania and uranium.

$$\frac{2}{2-x} \; UO_{2-x} \rightarrow UO_2 + \frac{x}{2-x} \; U$$

The elemental uranium could then dissolve in the cladding and produce higher concentration gradients. These gradients increased with time to give the high peak rates of diffusion. Depletion of the uranium precipitate source caused the decay of the diffusion flux. This physical picture is consistent

with the recently determined phase diagram for uranium-urania at high temperatures.[4] It should be further noted that temperature gradients should move the more volatile uranium to the cladding interface.

The effects of thermal cycling and shut down are again graphically illustrated on a run on UO_2 encapsulated in arc-cast molybdenum (Figure 5). This test clearly indicates that peak increases of uranium flux can be expected as a result of lowering of temperature or a shut down followed by testing at the previously established temperature. Figure 6 illustrates similar effects, but in this case, the molybdenum is a powder metallurgy product. A common feature in all the tests was a higher initial flux at the beginning of the experiment followed by a decay. This appears to correlate with expected oxygen loss and adjustment of fuel stoichiometry. Some of the microstructural changes observed are similar to those discussed for tungsten [3,8]. The salient differences between the Mo-UO_2 system and the W-UO_2 system were that grain growth of molybdenum in the diffusion "window" area was retarded by comparison with the growth observed in the body of the capsule. This may indicate that grain boundary contamination as a result of diffusion retards the grain growth in that area.

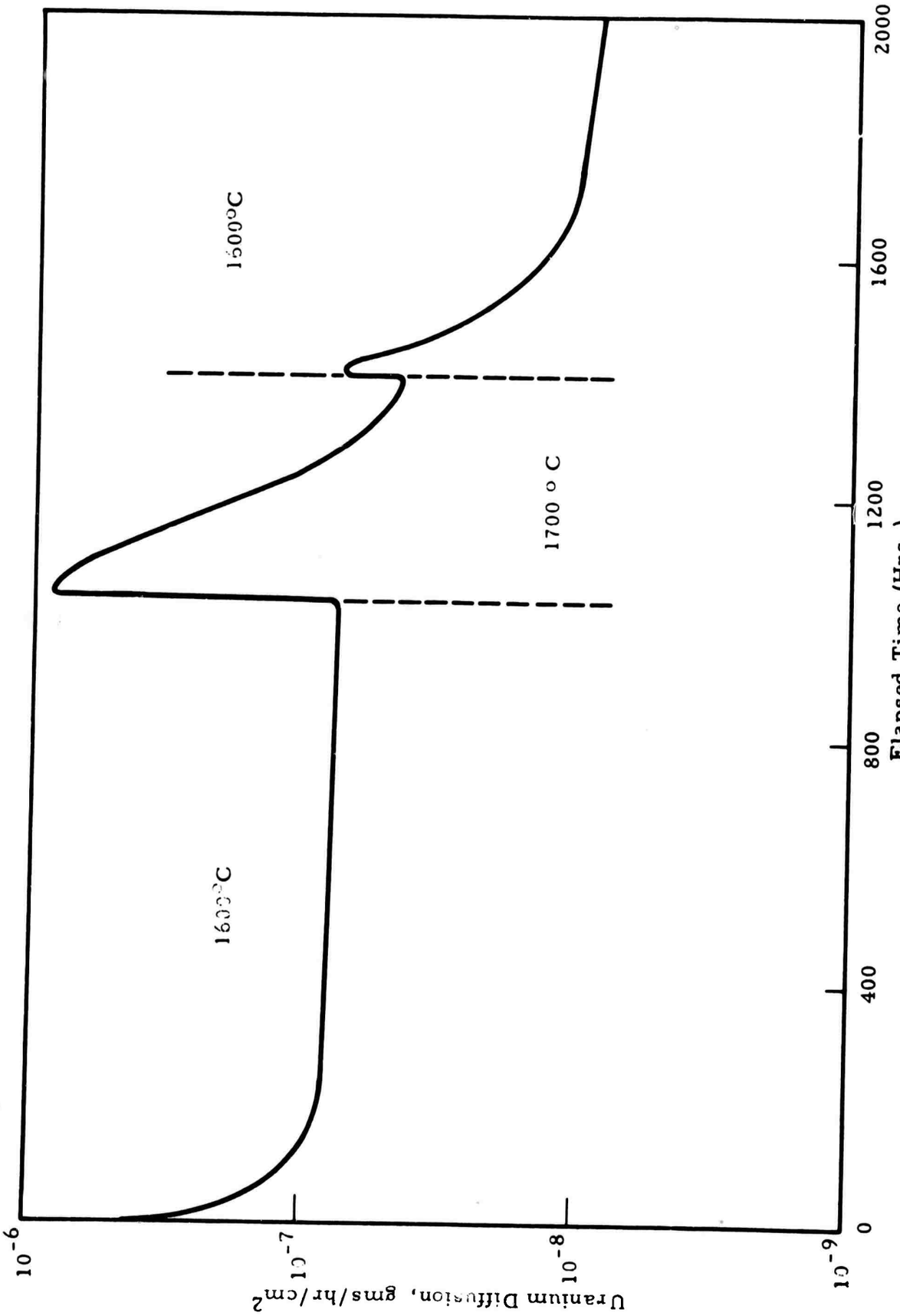

FIGURE 6. DIFFUSION OF URANIUM THROUGH POWDER METALLURGY SINTERED MOLYBDENUM

In all capsules, the urania was slightly hypostoichiometric. The capsule of Test 3* showed that most excess uranium was depleted in the fuel body. This means that uranium can migrate, dissolve in the cladding, and diffuse out of the system if the fuel is hypostoichiometric and is two-phase at the test temperature.

Conclusions

Several conclusions reached are: (1) Low diffusion rates of uranium through tungsten can be expected when tungsten is used to encapsulate urania between 1800 and 2200°C. The same observation applies to molybdenum between 1600 and 1750°C. (2) Surface contamination of tungsten is not a serious problem since the coverage amounts to approximately 1/100 of a monolayer. (3) It was found that powder metallurgy tungsten showed the lowest diffusion rate, followed in order by arc-cast and vapor-deposited tungsten. No definitive choice is available on molybdenum in terms of choice between arc-cast and powder metallurgy stock. (4) Thermal cycling can produce higher peak diffusion fluxes of uranium in molybdenum and tungsten capsules. (5) Hypo- and hyperstoichiometry in the fuel results in the enhancement of diffusion rates. (6) It is not likely that steady state fluxes measured will affect thermionic emission as already verified in UO_2-W [8].

Sub-task A-2 - Oxygen Diffusion Studies

General

The rate of diffusion of oxygen through the cladding of a molybdenum clad uranium dioxide thermionic emitter module may be important in determining the operating performance of the thermionic fuel element (TFE). At temperatures above 1600°C experimental evidence has shown[9-12] that uranium dioxide becomes substoichiometric yielding oxygen according to the reaction

$$UO_2 \quad UO_{2-x} + \frac{x}{2} O_2 \text{ (where } x > o). \qquad (1)$$

Slow diffusion of this oxygen through the Mo would probably not be deleterious to the operation of the TFE. Rapid diffusion of this oxygen through the cladding, however, would cause the formation of volatile molybdenum oxides at the emitting surface. The oxides could interfere with TFE performance by remaining as a gas in the interelectrode space or by depositing as a solid product. The degree of substoichiometry of the fuel also would increase by the loss of oxygen. On subsequent lowering of the temperature, disproportionation of the fuel would occur according to the reaction

$$UO_{2-x} \quad \frac{2-x}{2} \quad UO_2 + \frac{x}{2} U \quad \text{(where } x > o). \qquad (2)$$

The free uranium produced by this reaction could react with the molybdenum cladding. Because of the importance of the rate of oxygen diffusion in molybdenum, the present study

was undertaken. The diffusion coefficients (diffusivities) of oxygen through molybdenum were measured in the anticipated thermionic reactor operating temperature range, 1500 to 1800°C.

Two experimental techniques were used for measuring the diffusivity, D. The first approach involved passing a stream of oxygen gas over a molybdenum rod and analyzing the resulting gradient by using the non-steady state solution to Fick's second law for an infinite cylinder. Because of experimental difficulties with this method, a second approach was also used. In this method, the steady state gradient and flux of oxygen moving through a thin-walled-molybdenum cylinder were measured. The diffusivity was calculated using Fick's first law. Final determination of diffusivity values required the estimation of the solubility of oxygen in molybdenum as a function of temperature.

Experimental Procedure

Two methods were used to measure D, a "saturation" method and a "flux" method. Each technique is discussed individually below.

"Saturation" Method

The first method involved the determination of diffusivity by measuring the concentration gradient of oxygen in a cylindrical molybdenum rod subjected to treatment in

oxygen and comparing this gradient with that predicted by the solution of Fick's second law diffusion equation for an infinite cylinder.[13] (Details were given previously[14]). Initial plans required the uniform saturation of molybdenum rod samples, at a given temperature, to an oxygen concentration, C_o, in equilibrium with the maximum permissible external pressure o' oxygen. (C_o is also the concentration of oxygen at the surface of the rod at any time during exposure to the oxygen atmosphere). The saturation treatment was to be followed by a deoxidation treatment in hydrogen for a prescribed time. The resulting oxygen concentration gradient was then to be measured in the partially deoxidized samples. Calculations of saturation times based on values of D previously estimated from published low temperature data[15, 16] indicated that this procedure could turn out to be inordinately time consuming. Because of the possibility of excessive time for experimentation, the procedure of saturation followed by deoxidation was replaced by oxidation treatments only. This change was not expected to significantly affect the anticipated results.

A further simplification was introduced in the experimental procedure at this point which made it possible to determine D and C_o from experiments formerly designed to determine C_o.

One method of measuring C_o at a given temperature is to heat molybdenum rod samples of radius, a, in the maximum permissible oxygen pressure for different lengths of time, t. The average oxygen concentration, C_{av}, after a given time of exposure can then be measured and plotted as a function of time. As the time of exposure increases the oxygen concentration should asymptotically approach a maximum, or saturation value, C_o. The time required to reach C_o is called the saturation time. The curve of C_{av} vs t is called a saturation curve.

If C_o, C_i, (the uniform oxygen concentration in the samples before heating in an oxygen environment) and Dt/a^2 are known, a value for D can be found from the experimentally determined curve of oxygen concentration versus time (i.e., the saturation curve) be taking advantage of the following theoretical observation. It can be shown that each curve of the theoretical family of curves obtained by plotting $r\ C(r) - C_i \ / \ C_o - C_i$ versus r/a has a unique value of Dt/a^2 and the area under each curve A is unique. r is the radial distance from the center of the rod; C(r) is the oxygen concentration at r after a given time, t. Further, it can be shown that a given area is related to C_{av} of a particular rod by the following expression (see appendix A).

$$C_{av} = \frac{2(C_o - C_i)A}{a} + C_i \qquad (3)$$

This relationship permits the determination of D using a

method of successive approximations. This method is outlined below.

An estimate of D can be made from the saturation time indicated by the experimental saturation curve. The value of Dt/a^2 can then be calculated for each experimental point of the experimental saturation curve and the area under the theoretical curve corresponding to each Dt/a^2 value computed. Knowing A and having experimentally measured C_o and C_i, a theoretical value of C_{av} corresponding to each experimentally determined C_{av} can be found from equation (3). Plotting the theoretical C_{av} values vs time yields a saturation curve. This theoretical curve is then compared with the experimental curve. If the theoretical curve does not closely approximate the experimental curve a different value of D is estimated and the above procedure repeated until good agreement is obtained between the theoretical and experimental saturation curves. The value of D associated with the best fitting theoretical curve is the D for oxygen in molybdenum at that temperature.

To determine the experimental saturation curve at 1500 and 1800°C, 1/16-inch rods of molybdenum were heated in a mixed argon-oxygen atmosphere. The partial pressure of oxygen at a given temperature was kept approximately an order of magnitude below the equilibrium oxygen pressure for the formation of solid MoO_2[17] Oxygen partial

pressures used were 7.6×10^{-7} torr and 7.6×10^{-5} torr at 1500 and 1800°C, respectively. The samples were supported vertically within a water-cooled copper concentrator inside a vacuum chamber and inductively heated by an RF coil external to the vacuum chamber. Pressures were measured with a McLeod guage. Flow of the gas into the vacuum chamber was controlled mechanically with a micrometer needle valve. For a given oxygen pressure, micrometer settings varied only slightly from sample to sample. Sample temperature was measured with an optical pyrometer within $\pm 1\%$. A black body hole (0.020-inch diameter x 0.100-inch in depth) at the upper end of the sample and a black body hole in the molybdenum sample support were viewed for temperature measurements. Temperature uniformity over the length of the sample was kept within 20°C. The apparatus is shown in Figure 7.

Difficulties in maintaining a steady temperature at 1800°C eventually required the use of 1/8-inch diameter samples at that temperature to provide better electrical coupling between samples and the induction heater.

Rods of both diameters were given vacuum (approximately 10^{-6} torr) anneals prior to exposure to the oxidizing environment. The 1/16 and 1/18-inch diameter rods were heated at 1900°C for 7 and 28 hours, respectively. The

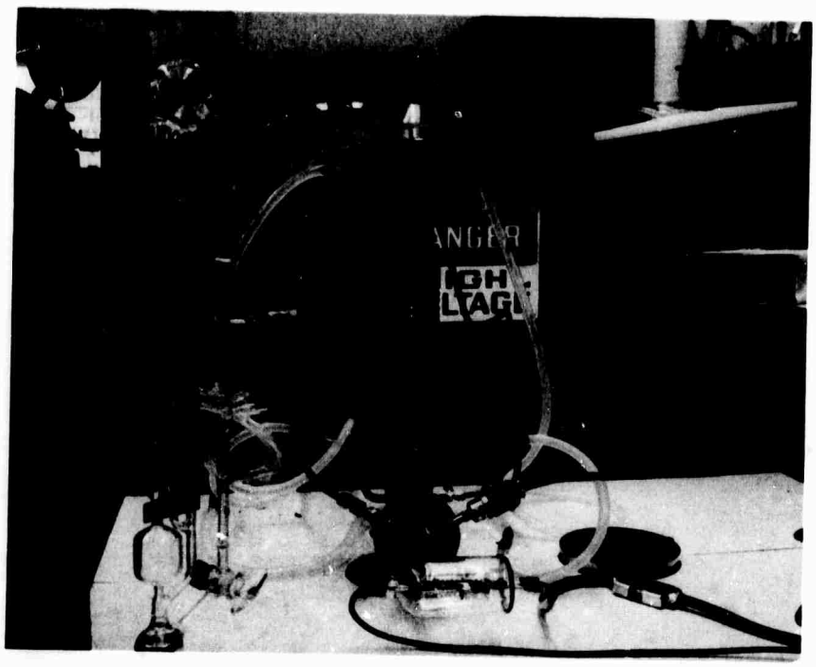

FIGURE 7. INDUCTION HEATING APPARATUS

purpose of the anneals was to reduce C_i to a low value and to change the wrought structures of the rods to uniform recrystallized structures. The post-anneal grain size of 1/16-inch diameter rods, however, was found to be quite variable. Photomicrographs of the samples before and after annealing are shown in Figure 8. The chemical compositions of the rods after annealing are presented in Table 4*. The precisions of oxygen and carbon analyses given in this report were ± 8 and ± 5%, respectively. Where more than one sample was analyzed for a given element, an average value and the individual values (in brackets) are given.

"Flux" Method

While continuing the above method for measuring the diffusivity of oxygen in molybdenum, a second technique was originated when scatter was found in the data to be used for determining the experimental saturation curve. According to Fick's first law,[18] the flux, J (gms/cm^2/sec), or quantity per second, of diffusion matter passing normally through an area, A(cm^2), under the action of a concentration gradient, dc/dx (gms/cm^4) is given by

*Oxygen analyses of samples were made by Luvak Incorporated, Newton, Mass. Carbon and nitrogen analyses were performed at National Research Corporation, Cambridge, Massachusetts.

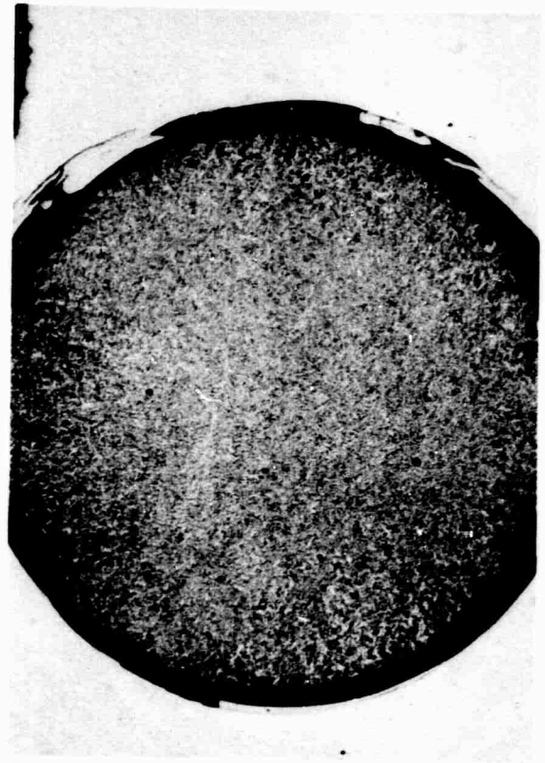

As-Received 50X

a. One Sixteenth-inch diameter Rod

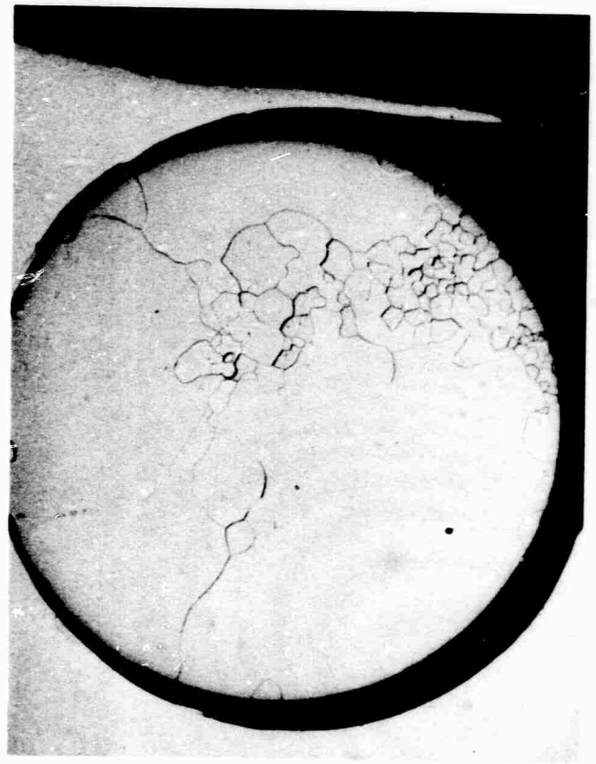

ETCHED 50X

b. One Sixteenth-inch diameter Rod After 7 Hours at 1900°C in Vacuum (10-6 torr)

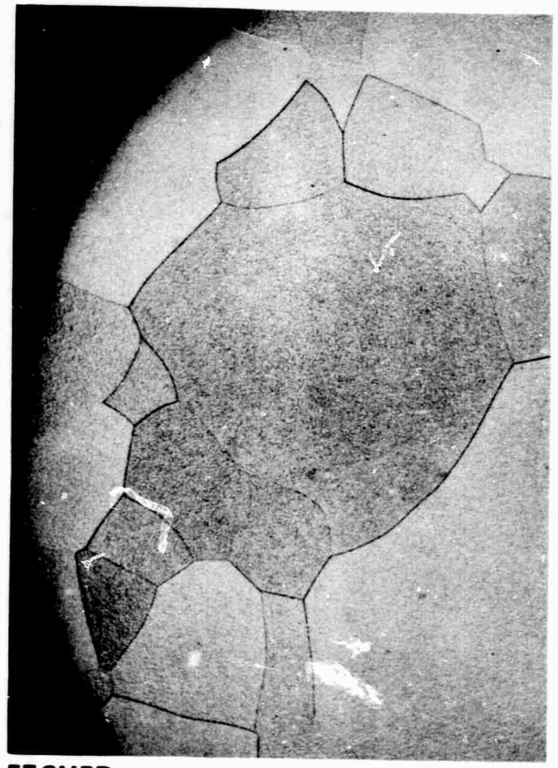

ETCHED 50X

c. One Eigth-inch Rod After 28 Hours at 1900°C in Vacuum (10-6 torr)

FIGURE 8. TRANSVERSE SECTIONS OF 1/16 INCH DIAMETER SINTERED AND 1/8 INCH ARC CAST MOLYBDENUM RODS. (IN 8a AND 8b THE SAMPLE IS THE WHITE CURCULAR AREA BOUNDED BY AN ANNULAR VOID AREA WHICH APPEARS BLACK).

TABLE 4.

Chemical Composition of Molybdenum Materials (ppm)

Element	Rods: 1/16-inch dia (a) (After Vacuum Anneal)	Rods: 1/8-inch dia (b) (After Vacuum Anneal)	Rods: 1/16-inch dia (b) (As-received)	Tube (c)	Caps (d)	Analytical Technique
O	4.9 (3.7, 7.7, 4.6, 3.7) 18	4.6 (6.0, 3.8, 3.9) 10	8 (8.5, 7.6, 7.8) 36	24	22	Vacuum fusion
C	(22, 13)	(11, 11, 7)	(44, 27)	52	211	Conductometric
N	< 10	< 5	< 5	n.d. (e)	n.d.	Kjeldahl
Al	10	30	< 10	< 1	< 1	Emission spectrographic
B	< 2	< 5	< 5	< 1	< 1	"
Ca	20	< 10	< 10	< 10	< 10	"
Cd	< 20	< 5	< 5	< 10	< 10	"
Co	< 2	50	< 10	< 5	< 5	"
Cr	100	100	< 10	< 10	< 10	"
Cu	10	< 10	< 10	< 1	< 1	"
Fe	50	500	< 5	10	10	"
Mg	1	5	< 0.1	< 1	< 1	"
Mn	1	1	10	< 1	< 1	"
Mo	Major	Major	Major	Major	Major	"
Na	50	< 50	< 50	< 50	< 50	"
Ni	5	< 10	< 10	< 10	< 10	"
Si	100	500	< 5	10	10	"
Sn	< 1	10	10	< 5	< 5	"
Ti	20	< 10	< 10	< 10	< 10	"
V	10	< 10	< 10	< 10	< 10	"
W	< 20	< 100	<100	<100	<100	
Zn	< 10	< 10	< 10	< 10	< 10	
Zr	< 2	50	50	< 5	< 5	

a - Sintered rod from General Electric Company

b - Arc cast rod from Climax Molybdenum Company

c - Sintered molybdenum from Cleveland Tungsten Company

d - Sintered rod - source unknown

e - n.d. = no determination

$$J = -D\frac{dc}{dx} \quad . \tag{4}$$

Solving (4) for D for a one-dimensional case gives

$$D = -\frac{\Delta x}{\Delta c} J. \tag{5}$$

It is assumed in equation (5) that diffusion is taking place in only one dimension and that D is independent of composition. Both assumptions are met in the experimental method described below. The diffusion flux passes through a thin walled cylinder (0.020-inch thick) which closely approximates one dimensional flow and the solubility of oxygen is < 100 ppm in molybdenum and thererfore D is independent of composition.

To measure D at a given temperature using the above relationship, thin walled sealed molybdenum capsules containing a fixed partial pressure of oxygen were heated in vacuum (approximately 10^{-6} torr). The flux was found by measuring the total weight loss rate per unit surface area of the capsule and correcting the weight loss for oxygen loss by mass spectrometrically determining the oxygen content of evaporating species. The concentration gradient was established by measuring the oxygen concentration of molybdenum rods contained inside and outside the capsule after the system had been heated for a length of time estimated to saturate the rods.

Test capsule preparation was as follows. Several 1/16-inch diameter molybdenum rods were placed in ultrasonically

cored holes of a sintered pellet of Mo + MoO_2 (approximately equal amounts of each) 0.55-inch long by approximately 0.4-inch diameter. The purpose of the pellet was to provide a partial pressure of oxygen within the capsule equal to the equilibrium pressure for the formation of solid molybdenum dioxide.[17] Under these conditions the maximum material solubility of oxygen in molybdenum at a given temperature could be attained at the inner capsule surface without nucleation of a second phase. The pellet was then sealed in a molybdenum capsule (0.45-inch od x approximately 0.6-inch long x 0.020-inch wall) formed by inert gas welding machined molybdenum lids to a molybdenum tube section. |All molybdenum parts were vacuum fired (approximately 10^{-6} torr) at 1500°C for one hour prior to assembly|. A leak check of the capsules with a helium mass spectrometer leak detector showed the capsules to be leak tight. A longitudinal and transverse section of a typical test capsule (after 400 hours at 1500°C) is shown in Figure 9. Photomicrographs of the as-received structures of the tube cap and rod are shown in Figures 10 and 11. Chemical analyses of the components are given in Table 4.

Two capsules were isothermally tested at 1500°C and two at 1800°C to measure weight losses and to establish the equilibrium concentration of oxygen in the rods. The tests were carried out in high temperature resistance heated vacuum furnaces. Temperature was regulated within ± 1% of the

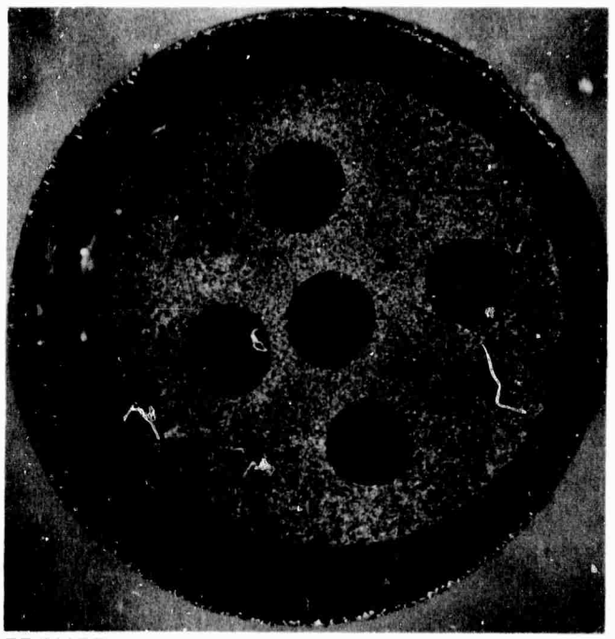

ETCHED 2.5X

a. Transverse Section

ETCHED 2.5X

b. Longitudinal Section

FIGURE 9. TYPICAL MOLYBDENUM DIFFUSION CAPSULE (NO. 3) CONTAINING PELLET OF MOLYBDENUM AND MOLYBDENUM-DIOXIDE AND MOLYBDENUM RODS, AFTER 400 HOURS VACUUM ANNEAL.

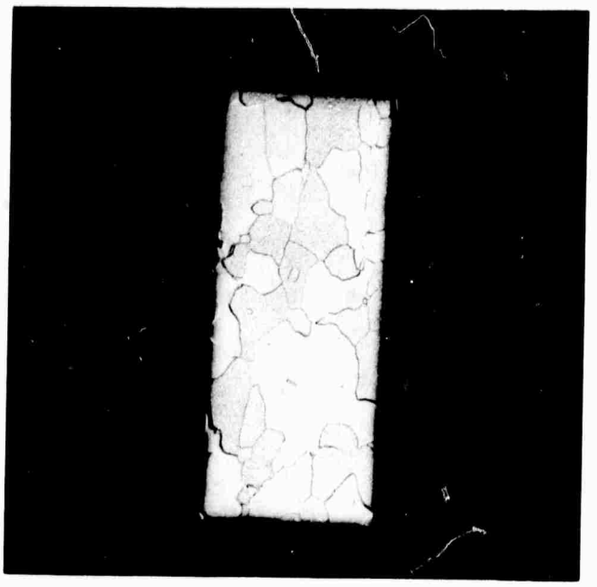

ETCHED 50X

a. Tube

ETCHED 50X

b. Cap

FIGURE 10. AS-RECEIVED STRUCTURES OF MOLYBDENUM TUBE AND CAP.

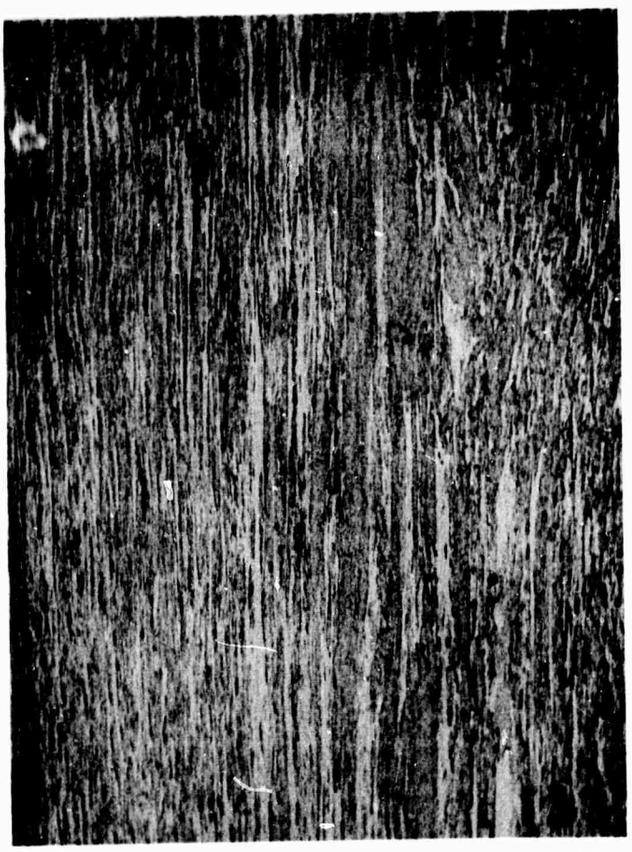

ETCHED 50X

FIGURE 11. AS-RECEIVED STRUCTURE OF 1/16 INCH DIAMETER ARC CAST MOLYBDENUM RODS USED INSIDE AND OUTSIDE OF DIFFUSION CAPSULES

desired test by tungsten/rhenium thermocouple control systems.

Mass spectrometric studies were made to determine evaporating species. Two additional capsules were tested in a Bendix Time-of-Flight mass spectrometer and the species determined at each temperature of interest.

Results and Discussion

"Saturation" Method

Results of tests to determine experimental saturation curves at 1500 and 1800°C are given in Figures 12 and 13. The number adjacent to each point is the sample number. The magnitude of the sample number indicates the relative chronological occurrence of the test, e.g., sample 1 was tested first. Weight loss associated with each sample is plotted as a function of time in Figures 14 and 15 for 1500 and 1800°C tests, respectively. The theoretical weight loss of molybdenum, based on Langmuir evaporation, i.e., the maximum rate of evaporation into a vacuum was calculated[19] and is also shown. The calculated loss of molybdenum is only 6×10^{-2} mg after 409 hours at 1500°C. It is obvious that molybdenum oxide must also have been forming and evaporating during tests at both temperatures. This mechanism would account for the additional material loss observed. The most likely gaseous specie is molybdenum dioxide. Appreciable reduction in sample diameter

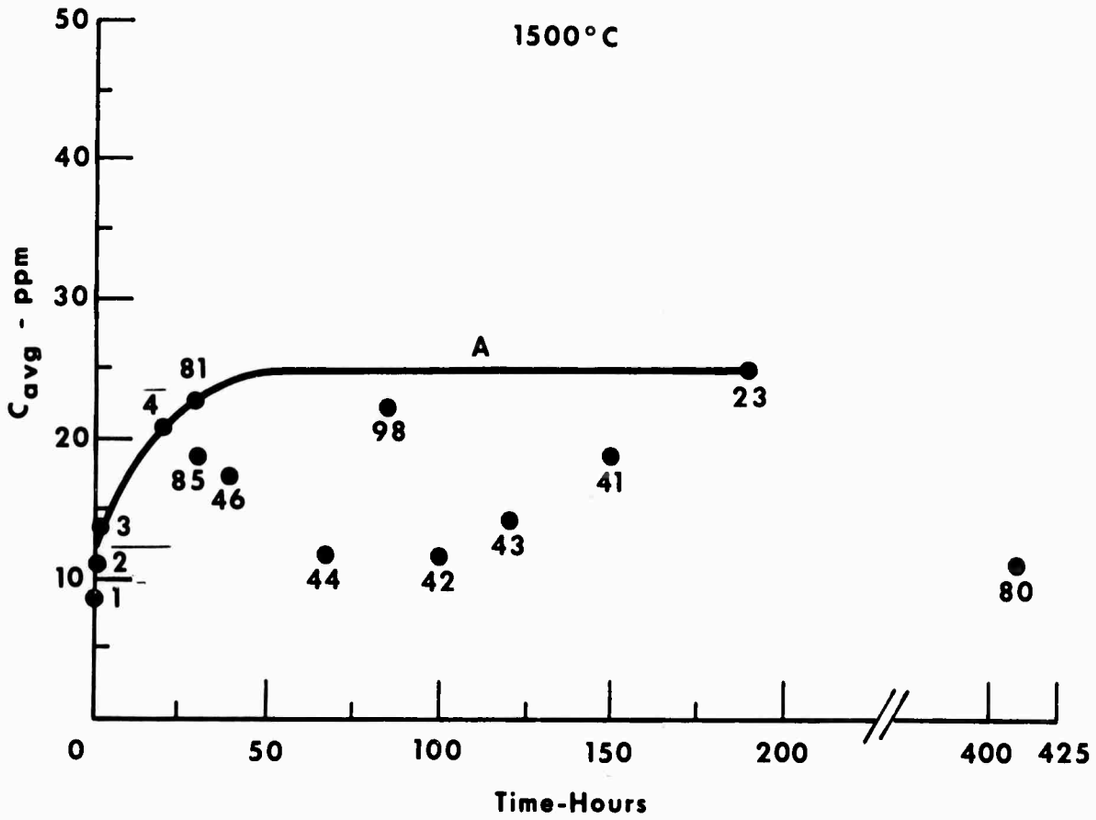

FIGURE 12. AVERAGE OXYGEN CONCENTRATION OF 1/16 INCH DIAMETER MOLYBDENUM RODS VS TIME AT 1500°C (Po_2 = 7.6 x 10^{-7} torr)

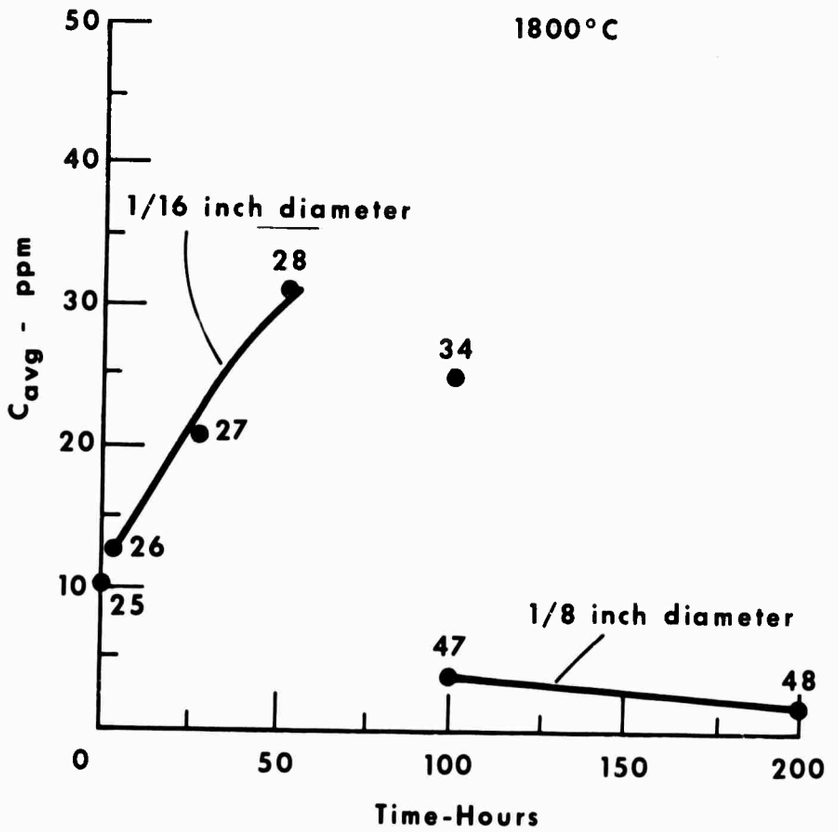

FIGURE 13. AVERAGE OXYGEN CONCENTRATION OF 1/16 AND 1/8 INCH DIAMETER MOLYBDENUM RODS VS TIME AT 1800°C (Po_2 = 7.6 x 10^{-5} torr)

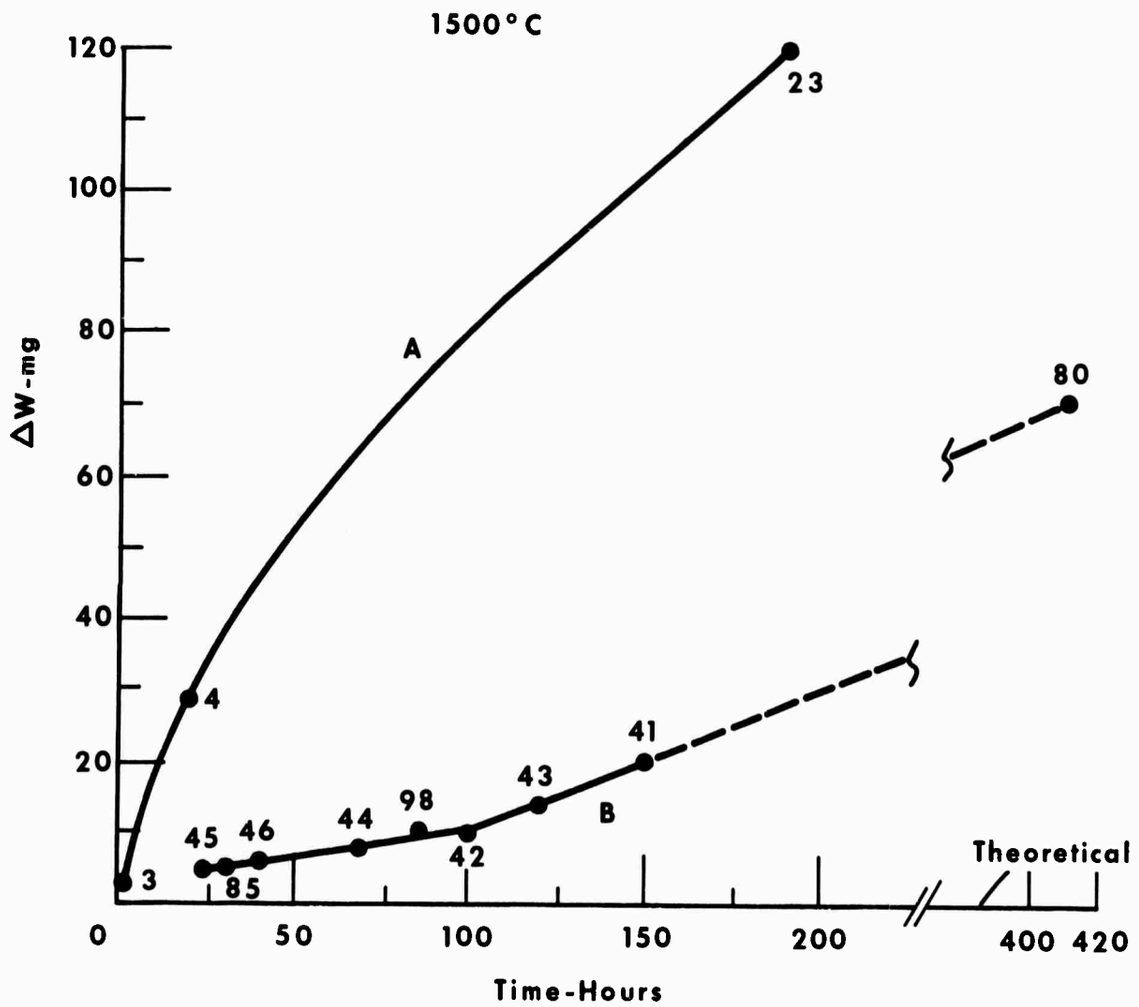

FIGURE 14. WEIGHT LOSS OF RODS VS TEMPERATURE AT 1500°C (Po_2 = 7.6 x 10^{-7} torr)

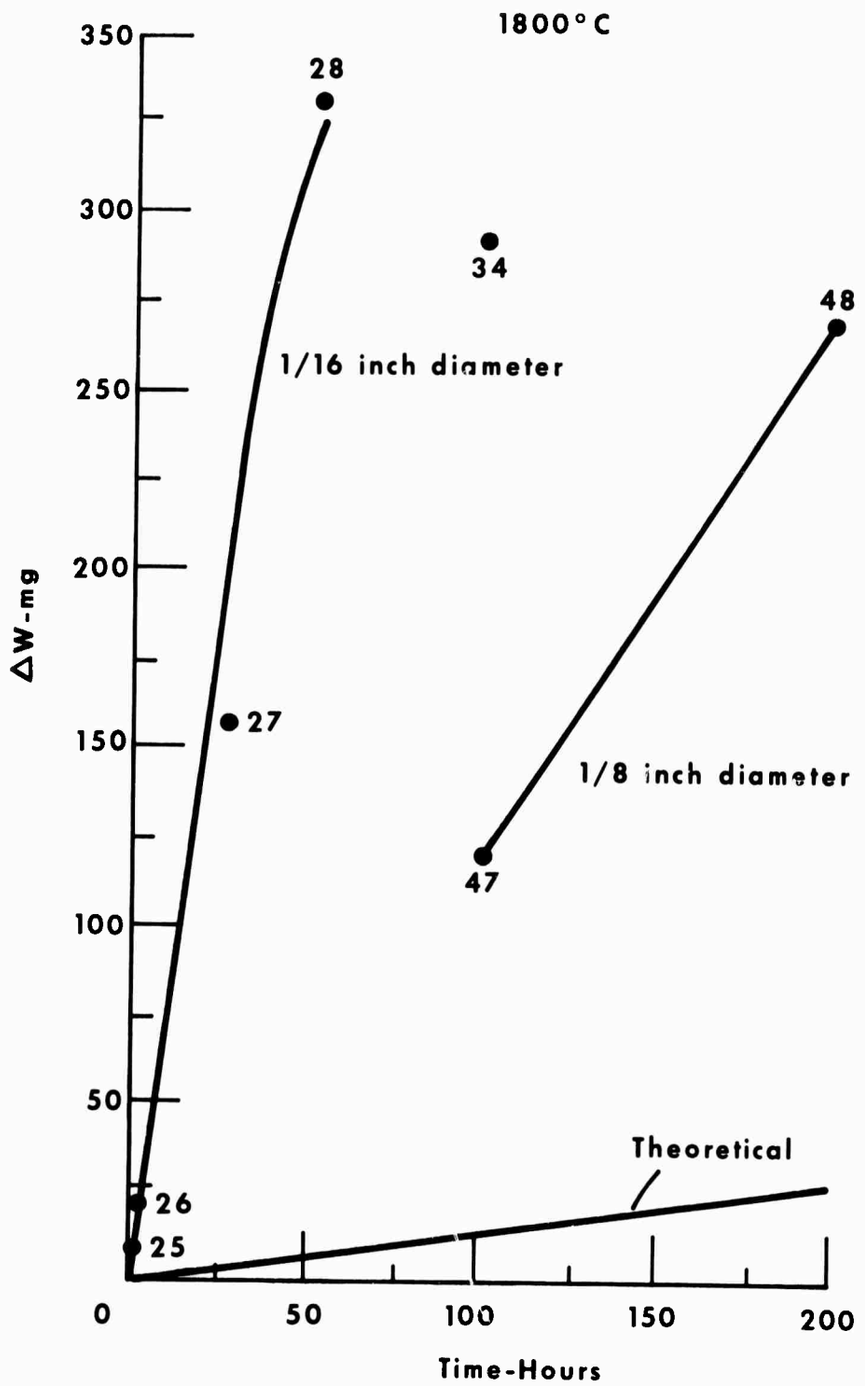

FIGURE 15. WEIGHT LOSS VERSUS TIME AT 1800°C
($Po_2 = 7.6 \times 10^{-5}$ torr)

did not occur until samples had been heated for 190 hours or more at 1500°C. At 1800°C, however, the diameter of sample 28 tested for only 52 hours, was reduced by approximately 0.010-inch (approximately 17% radial decrease), Figure 16.

As might be expected from the structure of the 1/16-inch diameter rods after their vacuum anneal (see experimental procedure), the 1/16-inch rods tested at 1500 and 1800°C exhibited highly variable grain size which could not be correlated with trends in C_{av} values of the samples. Etched structures of rods are shown in Figure 17. The 1/8-inch diameter rods showed huge equiaxed grains after annealing, some covering an entire transverse section. The results obtained at each temperature are discussed below.

1500°C Tests

The data of Figure 12 show considerable scatter, but the saturation curve determined by points 1, 2, 3, 4, and 23 was selected for analysis to evaluate D. This curve was selected because the five samples named were tested in the same experimental unit. Test number 81, carried out in a different apparatus, also falls on the curve based on the five most reliable tests.

Samples 1, 2, 3, 4, 23, and 46 were all tested in one vacuum induction apparatus. The rest of the samples were tested on a second apparatus different from the first only in one respect;

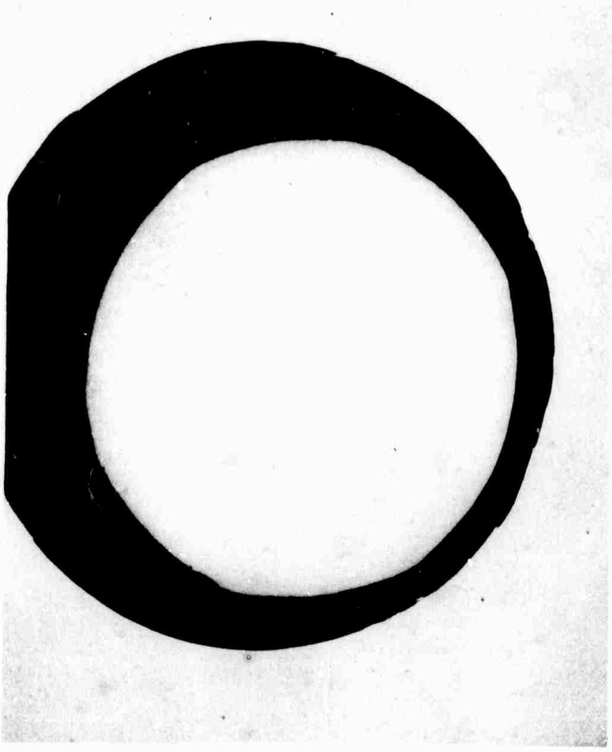

AS-POLISHED 50X

FIGURE 16. ONE SIXTEENTH-INCH DIAMETER ROD AFTER 52 HOURS AT 1800°C. SAMPLE 28.

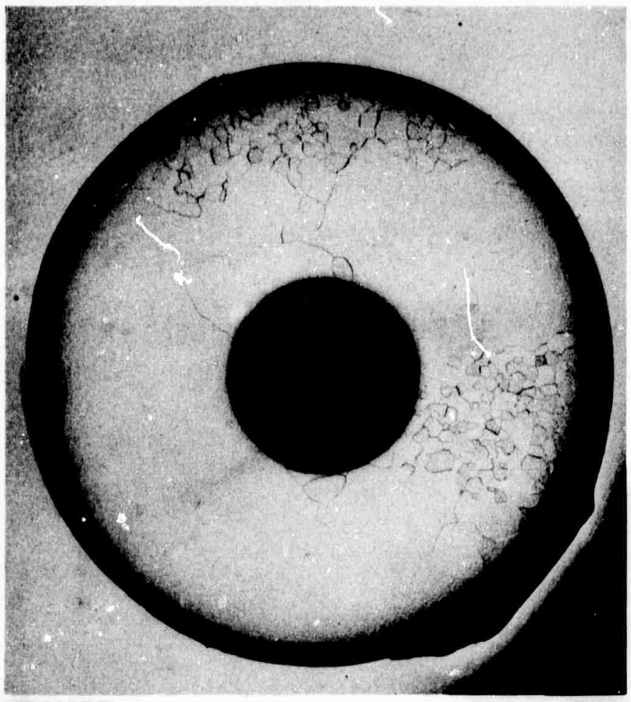

ETCHED 50X

a. 1500°C - 2 hours. White annular area is sample. Black circular area within sample is a black body hole.

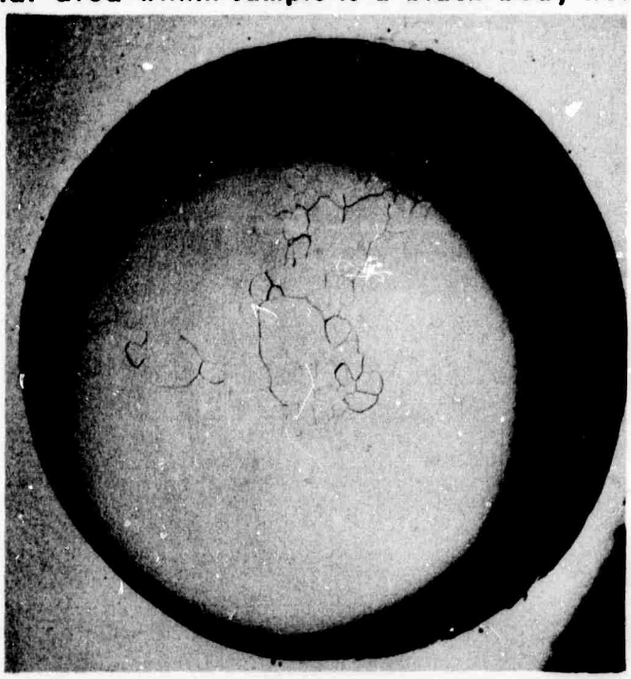

ETCHED 50X

b. 1800°C - 100 hours.

FIGURE 17. TRANSVERSE SECTIONS OF 1/16 INCH DIAMETER RODS AFTER EXPOSURE TO OXYGEN.

the second unit had a larger pumping speed and consequently a higher throughput of the argon-oxygen gas mixture to maintain the desired partial pressure of oxygen. The scatter of all data obtained after the initial series of runs (i.e., 1, 2, 3, 4, and 23) was so great that no attempt was made to construct a curve through them. The catter may have been the result of an acute sensitivity of C_{av} to small variations in pressure and/or flow rate.

The method of successive approximations outlined in the experimental procedure was applied to points 1, 2, 3, and 4. The C_{av} (25 ppm) of sample 23 was treated as C_o and the average oxygen concentration of rods before testing (4.9 ppm) was used as C_i. Calculated curves for a transfer coefficient, β, $= \infty$ (see appendix A) most closely approximated the experimental results. Of these, the curve for $D = 4 \times 10^{-8}$ cm^2/sec showed the best fit. Figure 18 displays the error band (shaded area) of the analytical oxygen values for the experimental points and curve A represents the calculated curve for $D = 4 \times 10^{-8}$. The saturation time, T_s, associated with curve A was approximately 43 hours. Since there was a possible error of $\pm$ 8% in the analytically determined value of any C_{av}, Co might also be as low as 23 ppm. The calculated curve, B, using the value of C_o yielded a better fot to experimental data. Values of D and T_s associated with curve B were 3×10^{-8} cm^2/sec and 53 hours, respectively. Using the other experimental extreme value of $C_o = 27$ ppm yielded a curve

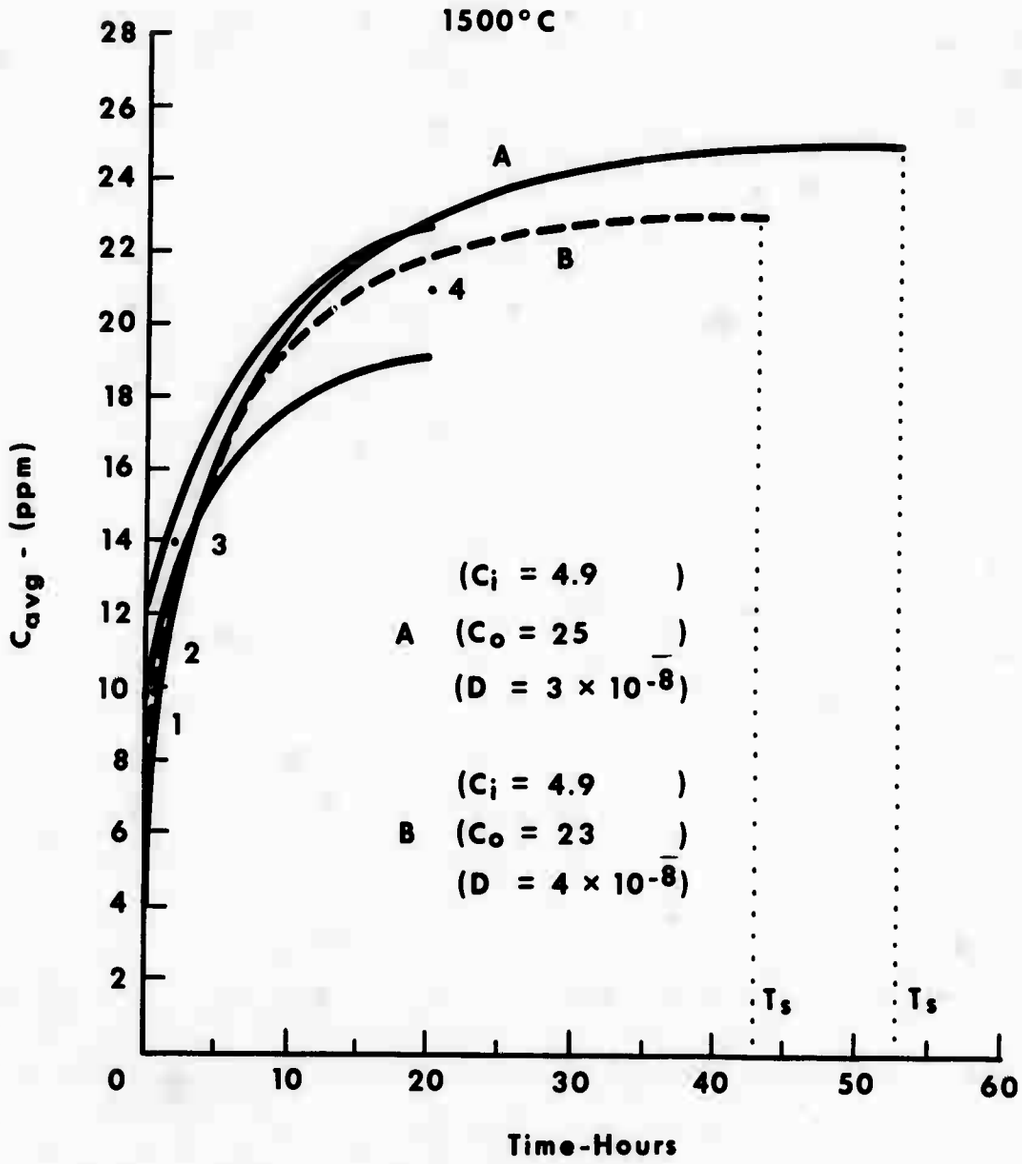

FIGURE 18. FITTING OF THEORETICAL CURVES, A AND B, TO EXPERIMENTAL DATA OF AVERAGE CONCENTRATION OF RODS VERSUS TIME AT 1500°C.

which did not fit the data as well as either curve A or B. One can expect that the value of D is known to about ± 50%.

1800°C

Experimental difficulties at 1800°C prevented determination of a saturation value using 1/16-inch diameter rods, Figure 13. (Point 34 is neglected in drawing the curve for 1/16-inch diameter samples because comparison with 1500°C data shows it to be unrealistically low). Results with 1/8-inch diameter samples were no more promising and no value of D could be measured. The C_{av} values for the 1/8-inch rods were quite low even though longer saturation times were required for these samples. The weight loss data for the 1/8-inch rods also seem low relative to the 1/16-inch diameter rods. These low values of C_{av} and weight are not as yet understood.

"Flux" Method

Limited success in determining D using experimental method I, led to the origination of method II described in the experimental procedure. This method involved the experimental evaluation of the various parameters related by Fick's first law. Results of vacuum anneals at 1500 and 1800°C are shown in Table 5. The annealing times were based on a very conservative estimate of the time it would take at a given temperature to saturate the 1/16-inch molybdenum rods inside the capsules. The weight

TABLE 5.

Vacuum Annealing Results

Capsule Number	Temperature (°C)	Time (Hours)	$\frac{\Delta W}{t}$* (gms/h)	Weight Loss Expected (gms)	Weight Loss Actual (gms)	Oxygen Concentration of Rods Inside (ppm)	Oxygen Concentration of Rods Outside (ppm)	Disposition
3	1500	400	0.0041	1.58	1.68	n.d.**	94	Metallography
4	1500	400	0.0035	1.35	1.17	39	22	Oxygen Analysis
1	1800	54	0.0864	4.46	1.04	n.d.	5.0	Metallography
2	1800	54	0.0986	5.09	1.01	13	4.8	Oxygen Analysis

* $\Delta W/t$ = average weight loss rate

** n.d. = no determination

loss rate was measured by weighing each capsule after each of a series of isothermal short term (1/2 to 2 hours) runs during the early stages of the vacuum anneal. The average weight losses calculated from these measurements are given in Table 5. If, following the short term runs, the weight loss rate for each capsule was maintained during the remainder of the isothermal anneals the expected weight loss would have been that shown in Table 5. The actual weight losses for the 1500°C capsules were close to the expected losses and indicated that oxygen was available inside the capsule during the entire vacuum anneal. The low actual weight losses for the 1800°C capsules indicated a loss of all the oxygen long before the completion of the 1800°C annealing treatments. X-Ray diffraction and metallographic analysis confirmed the expectations based on the weight loss data. Molybdenum dioxide was found in both 1500°C capsules but only molybdenum was found in the 1800°C capsules after testing. In the 1800°C capsule only a sponge of molybdenum was left where once there had been a pellet containing MoO_2 + Mo. Macrophotographs of capsules No. 3 and 1 are shown in Figures 9 and 19, respectively. The variable grain size of the molybdenum rods tested at 1500°C and the very large grains of the molybdenum rods at 1800°C are evident. Portions of the caps and walls of each capsule are presented in Figure 20 and 21. It was assumed in the concentration gradient calculation that no significant change occurred in the wall thickness of the capsules

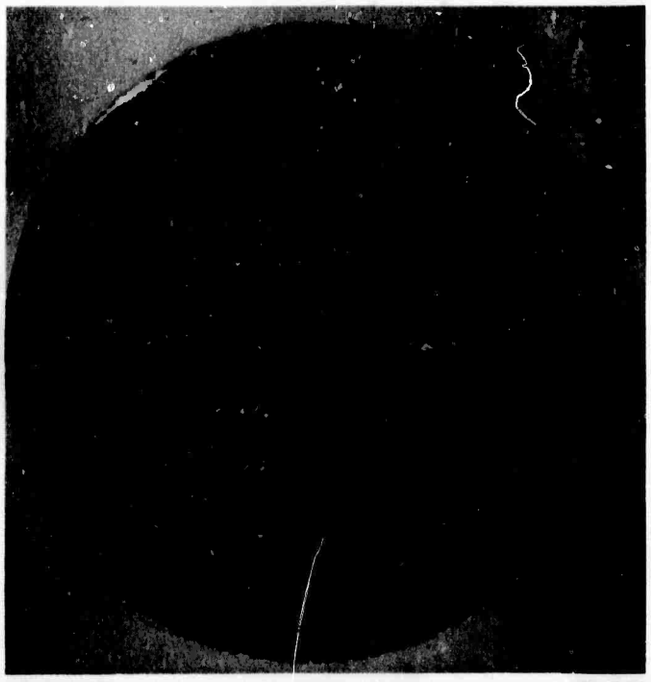

ETCHED 2.5X

a. Transverse section.

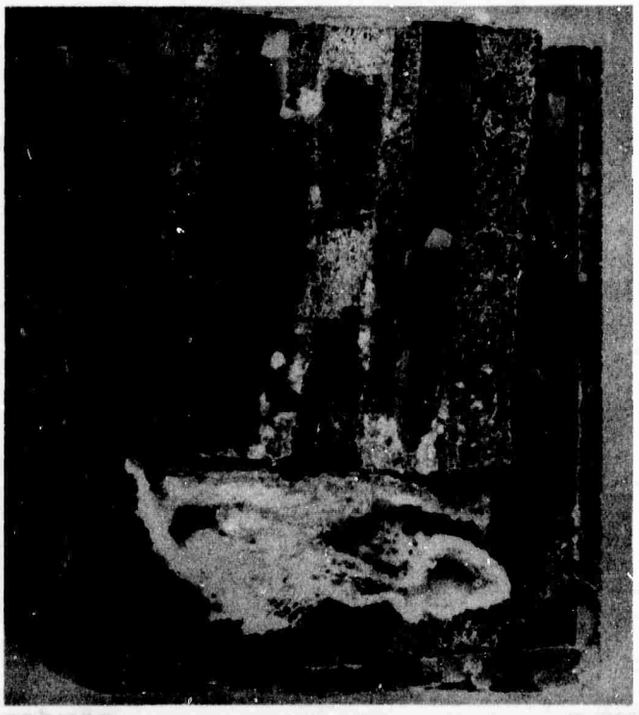

ETCHED 2.5X

b. Longitudinal section.

FIGURE 19. CAPSULE NO. 1 AFTER 54 HOURS AT 1800°C.

AS-POLISHED 50X

a. Capsule

ETCHED 50X

b. Wall

FIGURE 20. LONGITUDINAL SECTIONS OF CAPSULE NO. 3 AFTER 409 HOURS AT 1500°C.

AS-POLISHED 50X

a. Cap

ETCHED 50X

b. Wall

FIGURE 21. LONGITUDINAL SECTIONS OF CAPSULE NO. 1 AFTER 54 HOURS AT 1800°C.

during the initial test period, during which time the weight losses were being determined.

The oxygen content of the rods inside capsule No. 2 is obviously below the saturation value since all oxygen escaped from the capsule long before the end of the test. The oxygen content of the rods outside of capsules No. 3 and 4 are not accurate since a coating containing tantalum (high solubility for oxygen) was found on parts of the rods. The tantalum apparently evaporated from a surrounding support.

Two sealed capsules nearly identical to those used in the vacuum anneal studies were examined mass spectrometrically to discover the emanating vapor species between 1500 and 1800°C. Molybdenum, molybdenum oxide, molybdenum dioxide, and molybdenum trioxide were present up to 1700°C. Data above this temperature was not obtained because the two capsules ruptured during the tests. The average composition of the escaping oxygen species was $MoO_{2.1 \pm 0.5}$. The dominant specie was molybdenum dioxide.

The flux, J, was computed for capsules 1, 2, 3, and 4 from the known weight loss rate, evaporating species and the external geometric capsule surface area.

The concentration gradient for the 1500°C capsules was calculated assuming that the rods outside the capsules would have reached the same oxygen concentration as those outside the

1800°C capsules if tantalum had not masked their true values. Because of the loss of oxygen from the 1800°C capsules, a value for the oxygen concentration at the inside surface of the capsule wall for this temperature was estimated to allow calculation of the concentration gradient. (Appendix B). Diffusivity values calculated from Fick's first law using the flux and concentration gradient data discussed above were 5.34×10^{-8} and 4.79×10^{-8} cm^2/sec at 1500°C and 8.06×10^{-7} and 7.46×10^{-7} cm^2/sec at 1800°C. The error in the diffusivity values may be as large as $\pm$ 50%.

The activation energy for diffusion was determined to be 67,200 cal/mole from the slope of ln D vs 1/T, Figure 22. The activation energy is known within $\pm$ 20%. Values of D at 1600 and 1700°C were determined from Figure 16 to be 1.4×10^{-7} and 3.5×10^{-7} cm^2/sec, respectively. The diffusivity appears to increase by about a factor of 2 with every 100°C increase of temperature. This change is relatively small and indicates that it would be difficult to obtain reliable data at temperature intervals <100°C.

To obtain supplementary values of D in the 1400 to 1800°C range, evaluation of data obtained by Grossman, et.al.[11] was extended. In determining the compatibility of a capsule system of molybdenum clad $UO_{2.185}$, Grossman measured weight loss as a function of temperature as shown in Table 6. The weight loss was caused by the escape of excess

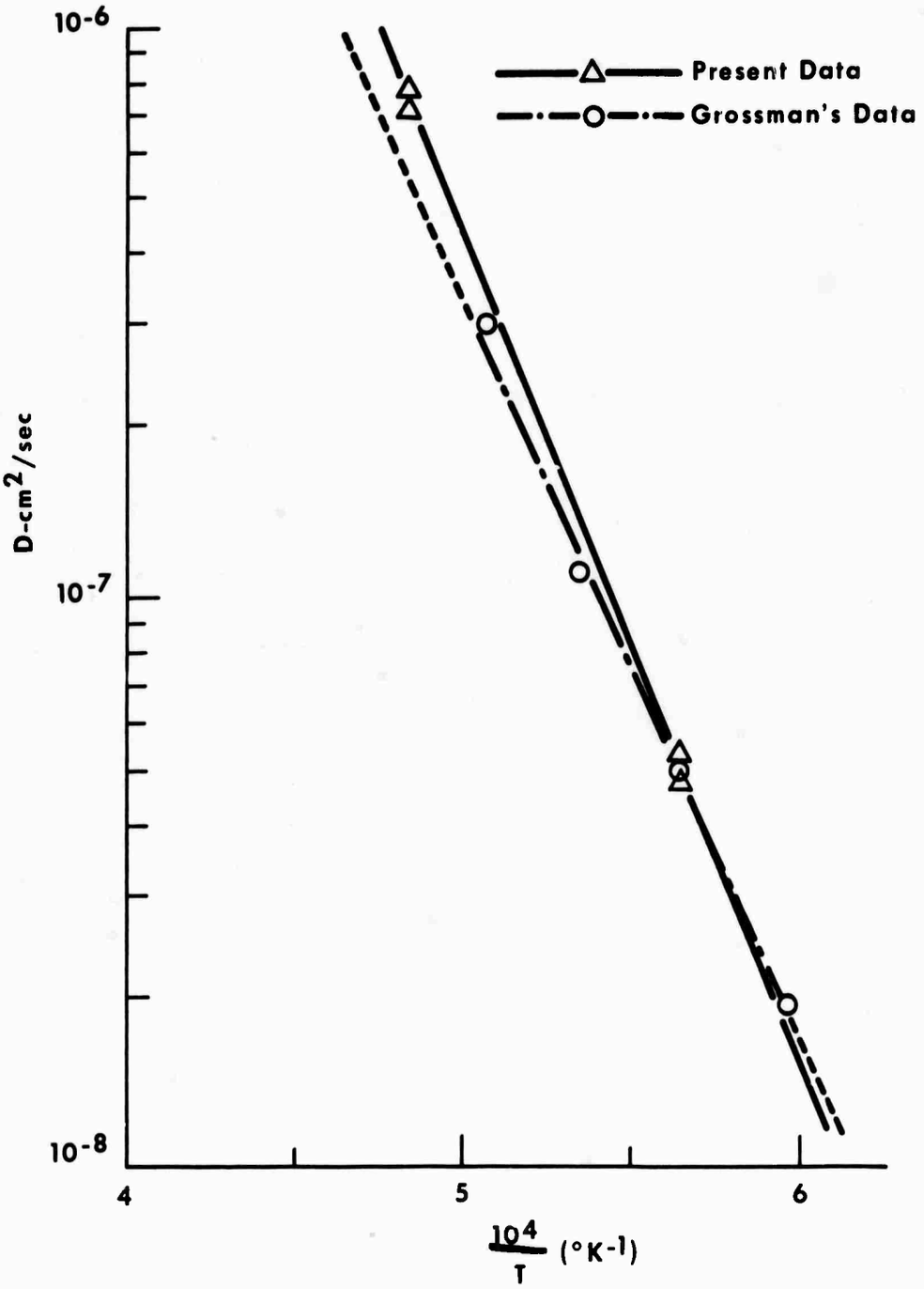

FIGURE 22. DIFFUSIVITY OF OXYGEN IN MOLYBDENUM VERSUS 1/T

TABLE 6.

Molybdenum-$UO_{2.185}$ Capsule Data[11]

Temperature (°C)	Time (Hours)	Weight Loss (mg)	0_2 Lost (mg)	$\frac{\Delta W}{t}$* (gms/h)	J (gms/cm^2/sec)	D (gms/cm^2/sec)
1400	3	4.2	1.05	3.5×10^{-4}	1.08×10^{-8}	1.92×10^{-8}
1500	3	13.1	3.25	11×10^{-4}	3.4×10^{-8}	4.97×10^{-8}
1600	3	35.7	8.4	28×10^{-4}	8.65×10^{-8}	1.10×10^{-7}
1700	3	103.7	25.7	85×10^{-4}	2.64×10^{-7}	3.06×10^{-7}
1800						5.4×10^{-7} *

* Extrapolated value.

of oxygen from the capsule. Grossman found that temperatures in excess of 1700°C were necessary to cause significant interaction between UO_{2+x} and molybdenum. Only trace amounts of molybdenum were found along the periphery of the UO_{2+x} pellet of a capsule tested to 1700°C. The concentration of oxygen at the inside capsule surface was believed to be close to the equilibrium value because molybdenum oxide was found over much of the inside surface. Because of the similarity of Grossman's study to the present work, the weight loss data of one of his capsules tested at various temperatures up to 1700°C were used to calculate values of D for oxygen diffusion in molybdenum. Assuming the average evaporating specie was $MoO_{2.1 \pm 0.05}$, weight loss rates and J were calculated at each temperature. Using the equilibrium values of the oxygen concentration in molybdenum as estimated in Appendix B, the diffusivity of oxygen in molybdenum was calculated for each temperature and is shown in Table III. The value for D at 1800°C was found by extrapolation of Grossman's data plotted as ln D vs 1/T (Figure 22). The activation energy, Q, for Grossman's capsule was found from this plot to be 59.6 Kcal/mole.

The diffusivity data reported above are summarized and compared in Table 7 with other diffusivity results on the molybdenum oxygen system found in the literature. In studying the effect of impurities on the welding of molybdenum, Platte[15] used

TABLE 7.

Comparison of Diffusivity Data

Temperature °C	Platte( ) D (cm^2/sec)	Brock( ) D (cm^2/sec)	Grossman( ) D (cm^2/sec)	Present Work Capsule D (cm^2/sec)	Present Work Rod D (cm^2/sec)
1400			1.85×10^{-8}		
1500	1.24×10^{-6}	2.48×10^{-9}	4.97×10^{-8}	5.34×10^{-8}	4×10^{-8}
				4.79×10^{-8}	3×10^{-8}
1600	2.4×10^{-6}	5.58×10^{-9}	1.10×10^{-7}	1.4×10^{-7} (b)	n.d.
1700	4.6×10^{-6}	1.17×10^{-8}	3.06×10^{-7}	3.5×10^{-7} (b)	n.d.
1800	8.3×10^{-6}	2.24×10^{-8}	5.7×10^{-7} (a)	8.06×10^{-7}	n.d.
				7.46×10^{-7}	
	Q (cal/mole)	Q (cal/mole)	Q (cal/mole)	Q (cal/mole)	Q (cal/mole)
	48,400	53,500	59,600	67,200	n.c. (c)

a - Extrapolated value.

b - Interpolated value.

c - n.d. = no determination.

limited data from a Battelle Memorial Institute report[20] to estimate Q at 1928°C as 48,300 cal/mole. In his calculation, Platte assumed the frequency factor, D_o, equaled 1 cm^2/sec. In a strain aging study on molybdenum, Brock[16] used the Cottrell[21] equation based on the Portevin-LeChatelier effect (assuming $D_o = 10^{-2}$ cm^2/sec) to estimate a Q of 53,500 cal/mole. The diffusivities shown in Table IV for each author were calculated by solving the arrhenius relationship for D assuming Q was temperature independent and using each author's selected value of D_o.

Stringer and Rudman have been studying the diffusivity and solubility of interstitials in molybdenum.[22] Their early results show a diffusivity of 10^{-8} at 1700°C and an activation energy of 54,500 cal/mole (assuming $D_o = 10^{-2}$ cm^2/sec) for oxygen. Because of the preliminary nature of this data, they concluded their agreement with Brock's values at 1700°C; "can only be regarded as an encouraging coincidence."

The diffusivities approximated from the literature are shown to indicate the order of magnitude of D one might expect in the temperature range of interest and to demonstrate the degree of uncertainty in the previous knowledge of D. Neither Platte nor Brock's studies were primarily addressed to the diffusion of oxygen in molybdenum and they only infer and/or postulate the diffusion parameters. The work of Stringer and Rudman is specifically aimed at measuring the diffusion parameters, but

conclusions based on their early results would be premature. A point adding some confusion to the results of the above authors is the value of D_o chosen for calculating Q. For example, had Platte used $D_o = 10^{-2}$ cm^2/sec to calculate Q, he would have obtained an activation energy of 28,150 cal/mole. Powers and Doyle[23] measured D_o as 10^{-2} cm^2/sec in the group-V metals, while Jacobs[24] found a value of 1.3 for D_o for oxygen diffusion in tungsten. Both values of D came from internal friction measurements. It seems likely that the value of D_o for group-VI metals would be greater than that for the group V.

The values of D experimentally determined in the present work by the flux and saturation method, fall midway between those of Platte and those of Brock and Stringer and Rudman. The D values determined from the present work are considered more reliable than those estimated from published literature for a number of reasons. The present studies were specifically designed to measure the diffusivity of oxygen through molybdenum at high temperature. The experimentally determined values at 1500°C are in very good agreement even though they resulted from three distinctly different types of experiments. Also, good agreement was obtained at 1800°C between the capsule experiments of the present work and Grossman's data.

Of the two flux experiments, the present work is considered more accurate than Grossman's because the present capsule tests were specifically performed to measure D and were

carried out under conditions most closely a
a steady state.

The diffusivities reported above were actually apparent bulk diffusivities in that the contribution of grain boundaries, if any, was neglected. The rate of diffusion along grain boundaries is generally more rapid than through the bulk of a given material. Diffusivities measured in polycrystalline material thus tend to be higher than the true bulk value. For the capsule tests, the contribution of the grain boundaries to the diffusion rate was probably low, if significant at all, because of the large molybdenum grains (ASTM 2-3) and the high test temperatures (i.e., at high temperature the difference between rate of bulk and grain boundary diffusion decreases and the bulk contribution tends to overpower the grain boundary contribution).[25]

The accuracy of the diffusivities derived from the capsule tests is somewhat limited by the small number of samples tested. As mentioned previously, however, the calculated diffusivities were corroborated by the results of at least one other experimental approach. The accuracy of the diffusivities depend, in part, on the correctness of the concentration gradient estimates (Appendix B). More precise values of the rate of diffusion of oxygen in molybdenum may be possible when the solubility of oxygen in molybdenum as a function of temperature is known. Q was calculated from

the slope of the curve resulting from plotting ln D vs 1/T. The accuracy of the Q value thus depends on the accuracy of D. More precise values of D should therefore yield better values of Q.

Conclusions

The diffusivities and activation energy for the diffusion of oxygen through polycrystalline molybdenum were determined in the temperature range 1500 to 1800°C. These values, which depend in part on an estimate of the solid solubility of oxygen in molybdenum as a function of temperature, were 67.2 ± 20% Kcal/mole for Q and the diffusivities were as shown below:

Temperature °C	D (cm^2/sec)
1500	$5.1 \times 10^{-8} \pm 50\%$
1600	$1.4 \times 10^{-7} \pm 50\%$
1700	$3.5 \times 10^{-7} \pm 50\%$
1800	$7.8 \times 10^{-7} \pm 50\%$

The activation energy determined is somewhat higher than than the values reported in the literature.

The values of D, however, fall roughly midway between the values estimated from or given in the literature and are believed to be more reliable than the literature values.

TASK B - Insulator Materials Development [35]

General

For a metal plus oxide system, chemical stability can generally be assured if the free energy of formation of the oxide is more negative than that of any solid oxide of the metal. If volatile products are produced, stability may still be maintained in an isothermal closed system. However, in an open system or in a temperature gradient, a reaction yielding a volatile product is favored with increasing temperature. The interaction between alumina and niobium is a reaction which yields both volatile and solid products.

Niobium is used with alumina in structural and in ceramic-to-metal seal applications because of the close match between their thermal expansivities. Alumina-niobium seals have been developed for use at 1200°C for nuclear thermionic converter application.[26] The long term stability of the alumina-niobium combination at high temperature has been in doubt due to the chemical similarity between niobium and tantalum. Ackerman and Thorn[27] have shown that tantalum enhances the evaporation of alumina through the reaction $Al_2O_3 + Ta = Al_2O(g) + TaO_2(g)$ plus other gaseous products. They point out that at high temperatures, the weight loss of a tantalum cell containing alumina was essentially the same whether or not an effusion hole existed in the cell; it can be concluded that at least one of the product species leaves the cell after diffusing through the tantalum walls.

Experimental Procedure

28

The niobium-alumina reaction was studied via the Knudsen method. Tungsten effusion cells containing an equimolar mixture of niobium and alumina were electron bombardment heated as shown in Figure 23. The Knudsen cell effluent was directed into the ionization source of a Bendix Time-of-Flight mass spectrometer. The cell chamber was valved from the spectrometer to facilitate sample change without breaking vacuum. Temperature capability of the cell heating system has been demonstrated to 2600°C.

The Knudson cell chamber was differentially pumped with two 8 l/s ion pumps which also monitored the total cell pressure. The pressure in the source region of the mass spectrometer was monitored with a Bayard-Alpert type ionization guage. The mass spectrometer vacuum was maintained by a mercury diffusion pump which was baffled from the spectrometer with Freon-cooled and liquid nitrigen-cooled baffles. Typical source pressure was 2 to 8 x 10^{-8} torr; cell chamber total pressure was between 2 x 10^{-7} and 5 x 10^{-6} torr during experimentation.

Sample temperature was measured by sighting into the effusion hole with an optical pyrometer. The pyrometer was calibrated against an NBS secondary standard tungsten strip lamp between 900 and 2300°C. Calibration has been extended to 3000°C by the rotating sector disk technique. Sample

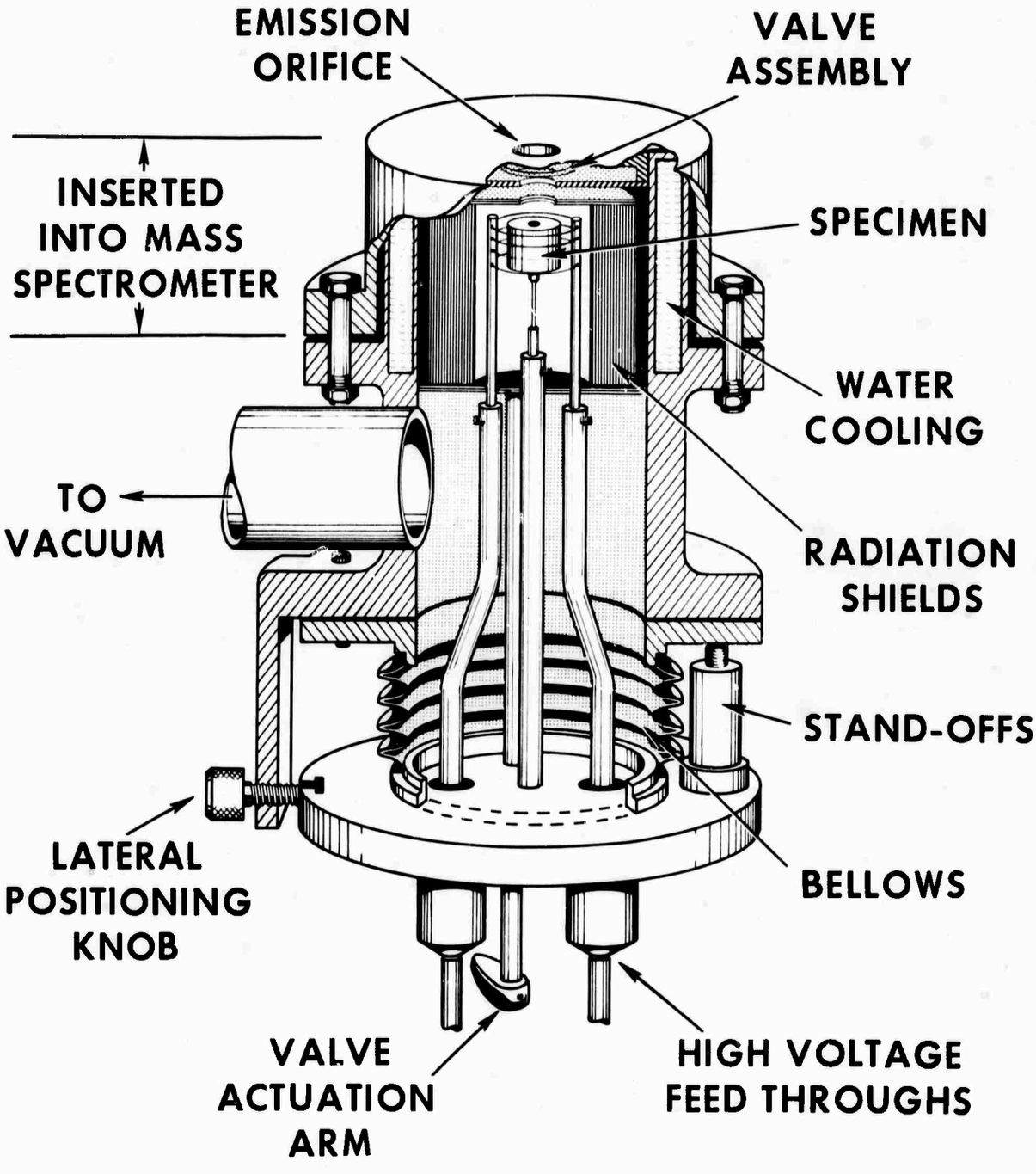

FIGURE 23. KNUDSEN CELL AND ELECTRON BOMBARDMENT HEATER ASSEMBLY

temperature was maintained constant to within $\pm 5^{\circ}C$ by the electron bombardment power supply. A mock-up of the Knudsen cell and its heater outside the mass spectrometer revealed no detectable temperature gradients over the cell.

Starting materials were powders which were pressed into low density pellets and fired at $1500^{\circ}C$ for 1 hour at 4×10^{-6} torr. The starting alumina contained less than 100 ppm total impurities (principal impurity cations were silicon and iron). The starting niobium contained <400 ppm metallic impurities, but had the following interstitial impurity content: 400 ppm nitrogen, 1800 ppm oxygen, 27 ppm hydrogen, and 340 ppm carbon. The oxygen content of the starting niobium was confirmed at 4000 ± 3000 ppm by X-Ray determination of the lattice parameter; the oxygen was presumed to be in solid solution in the starting metal since no other phases were detected.

In addition to the elucidation of gaseous products, chemical, metallographic, and X-Ray analyses were made of the starting materials and of the solid residue after each spectrometer or weight loss experiment.

Experiment Results

The relative abundance of various mass species observed over niobium plus alumina is shown in Figure 24. The

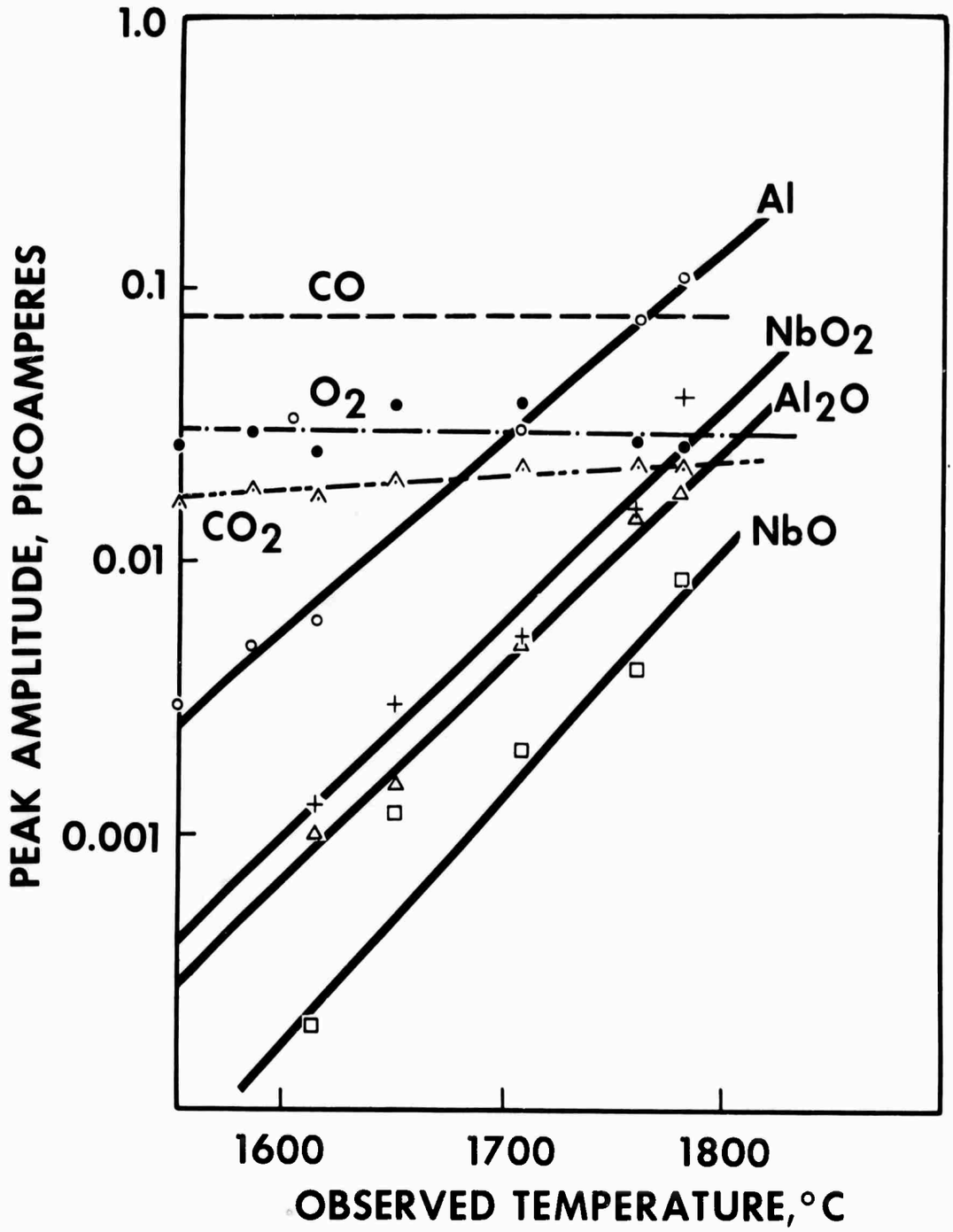

FIGURE 24. MASS PEAK AMPLITUDE VERSUS TEMPERATURE FOR NEUTRALS ABOVE $Nb+Al_2O_3$

common gas species originated in the cell heater assembly, not inside the Knudsen cell.

The mass peak intensities shown in Figure 24 were obtained after 3 days continuous heating between 1200 and 1600°C. All other mass peaks were at most one-tenth as intense as those shown in Figure 24 for any temperature. No significant changes in the relative intensities were observed after 2 more days of heating above 1500°C. Both neutral and ionized species were observed entering the source region. Figure 25 shows the temperature dependence of the ionized species. No other ionized species were observed. The relative amounts of ionized and neutral species changed when the specimen position was changed; the ions were apparently created by collisions between neutrals and electrons from the bombardment filament. No corrections to the observed intensities have been made for ionization efficiency or instrumental factors.

Residue in the Knudsen cells was analyzed by X-Ray diffraction and found to consist of three phases. Alumina was present with no change in its lattice parameter; niobium with 5000 ppm oxygen in solution[29] (a_o = 3313 Å ± 0.005) was found; and a new phase, niobium oxide, was present (a_o = 4.212 Å ± 0.009). The residue was examined metallographically and the three phases were seen. To bring out the niobium oxide precipitates in niobium, a metallographic procedure after Inouye[30] was followed.

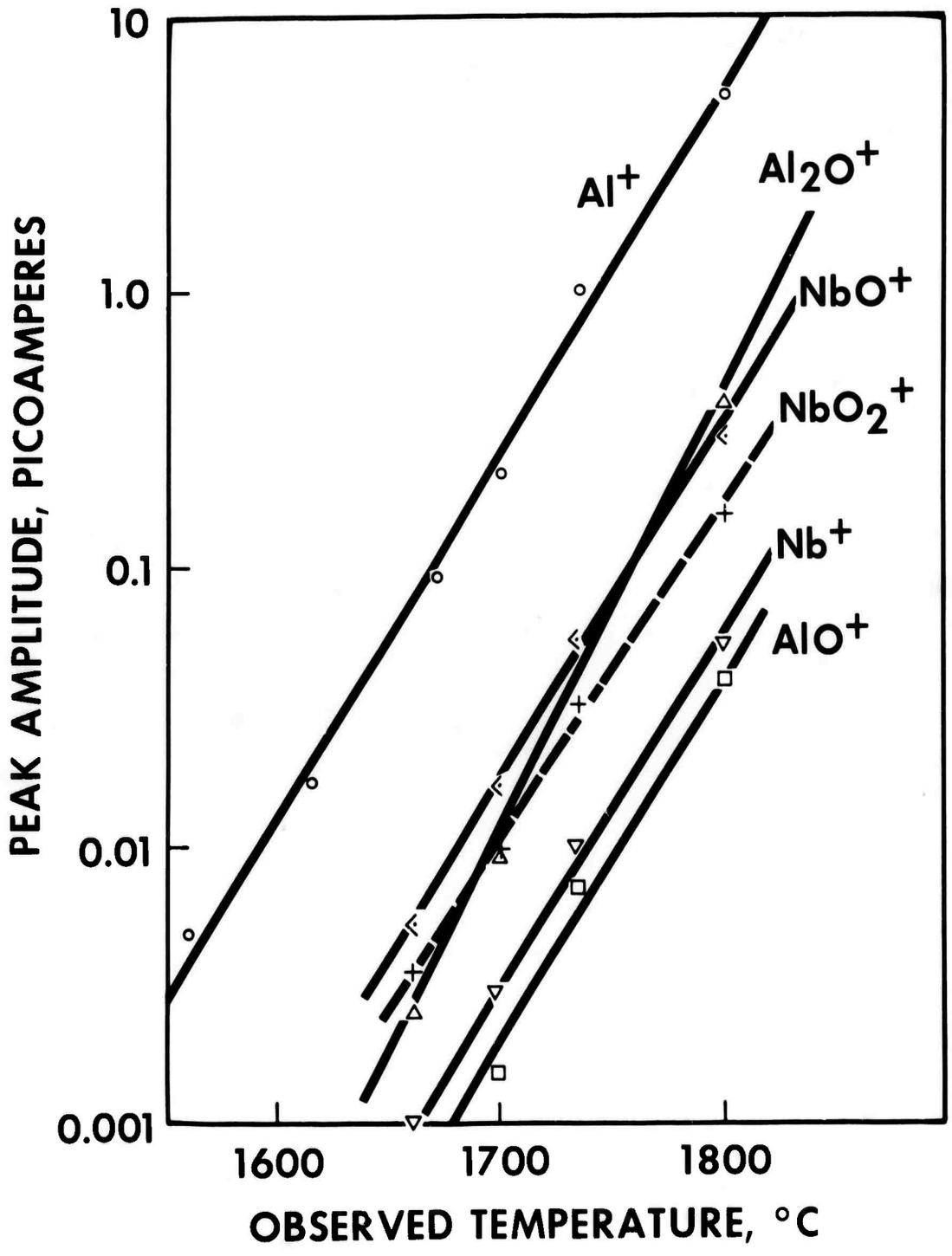

FIGURE 25. MASS PEAK AMPLITUDE VERSUS TEMPERATURE FOR IONS ABOVE $Nb+Al_2O_3$

The vapor species leaving a cell containing only alumina were also examined mass spectrometrically. The species 0(g), Al(g), and 0_2(g) were observed in the ratios 1:0.5:0.15 between 1570 and 2000°C. No corrections for ionization efficiency or instrumental factors have been made to the observed ratios.

The observed weight loss rate of a tungsten Knudsen cell containing niobium plus alumina is shown in Figure 26. The data in Figure 24 includes a Clausing correction factor of 1.32 for the impedance of the effusion orifice.[31]

Discussion

The principal species observed mass spectrometrically and the pressures of these species as found by weight loss rates agree well with the pressures calculated from existing thermodynamic data.[32] Three reactions which yield volatile species in excess of those found over alumina under neutral conditions are:

a. $Al_2O_3 + Nb = Al_2O(g) + NbO_2(g)$

b. $Al_2O_3 + 3Nb = 2Al(g) + 3NbO(s)$

c. $Al_2O_3 + 2Nb + 1/2\ O_2 = NbO(s) + Al_2O(g) + NbO_2(g)$

Reaction (c) is the sum of reaction (a) and the oxidation of niobium to form niobium oxide(s). Reaction (c) is limited by the oxygen available over niobium + niobium oxide(s) as shown in curve C of Figure 27. Figure 28 shows the calculated

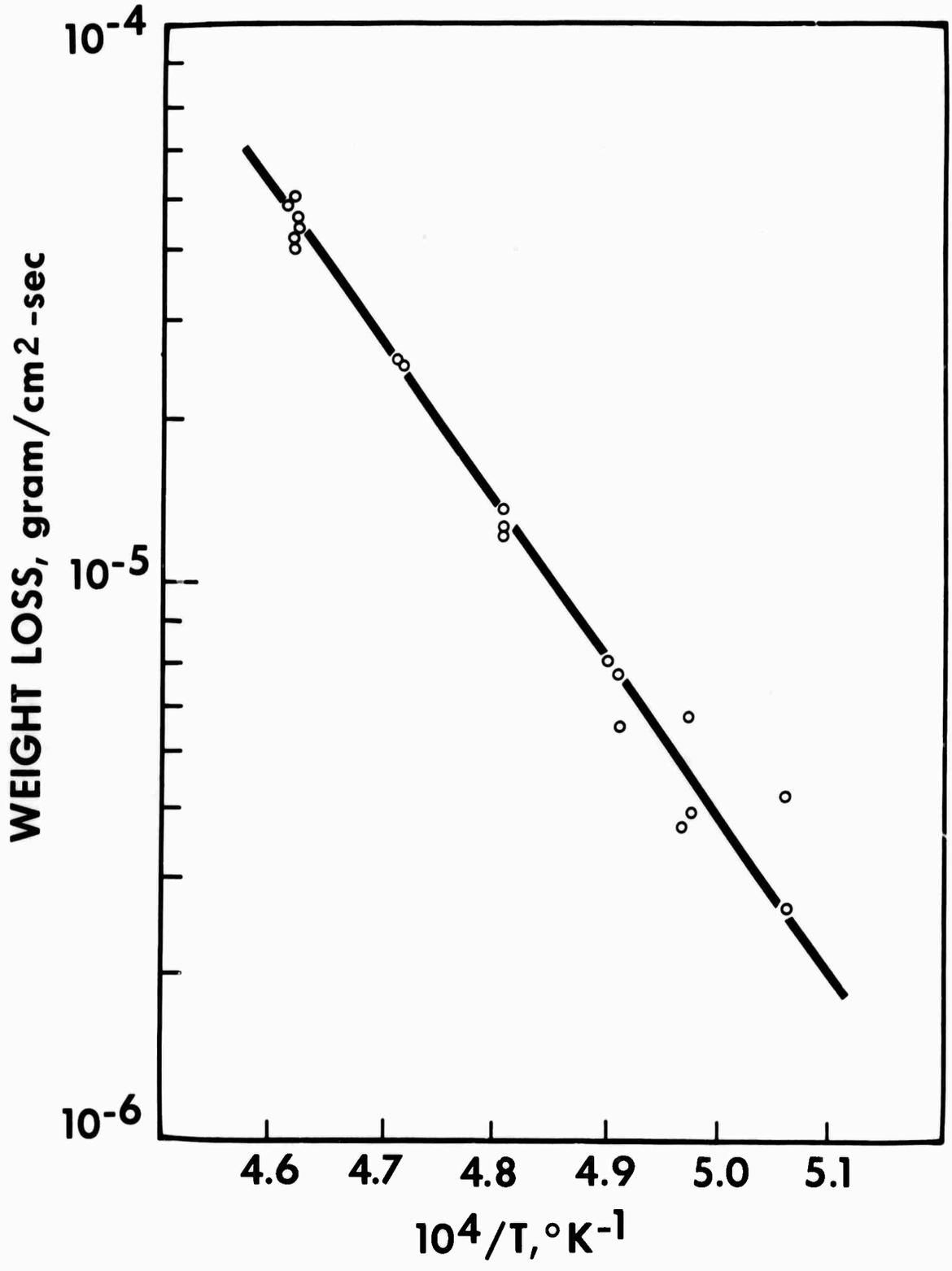

FIGURE 26. EQUILIBRIUM WEIGHT LOSS RATE OF $Nb+Al_2O_3$ VERSUS TEMPERATURE

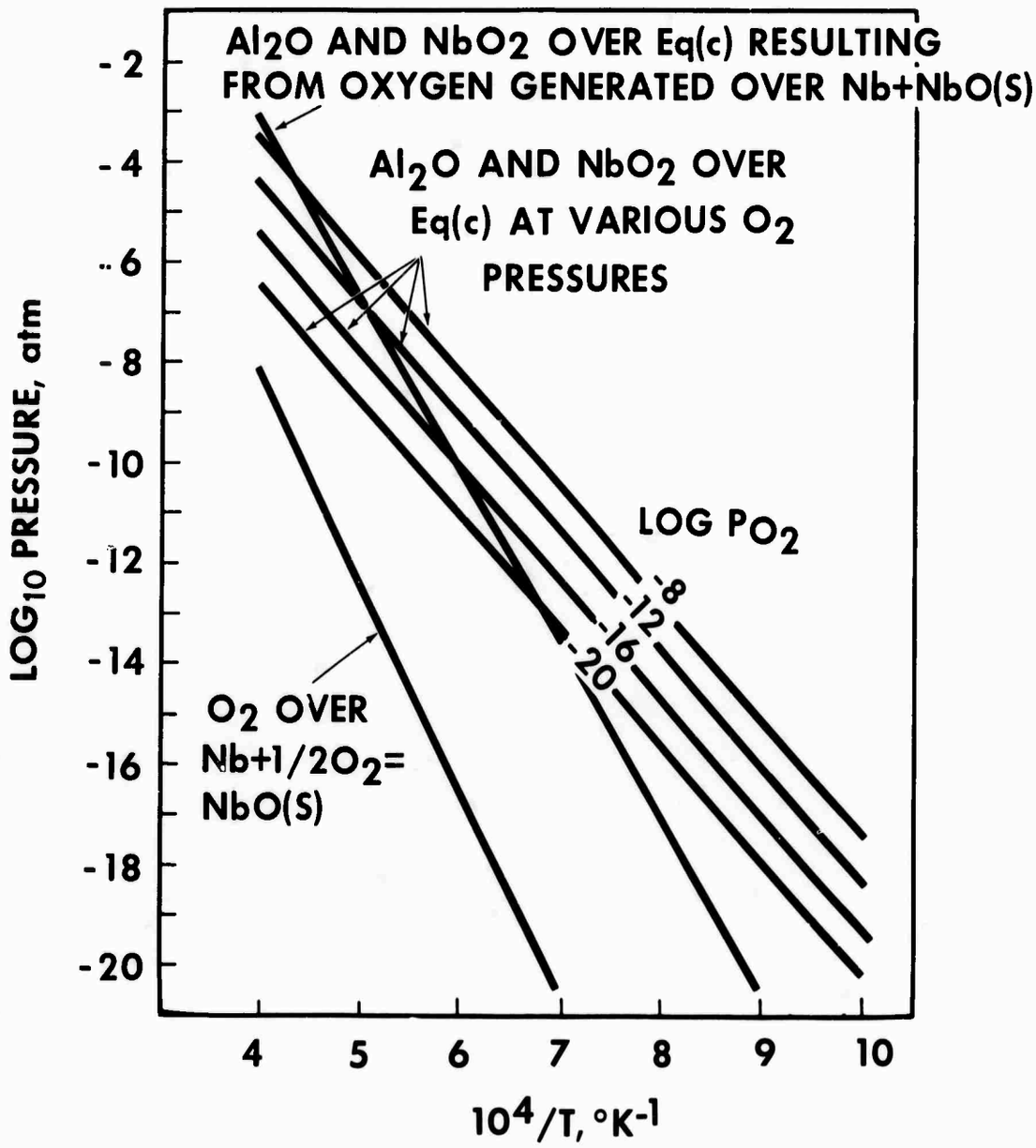

FIGURE 27. CALCULATED PRESSURES OVER REACTION (c)

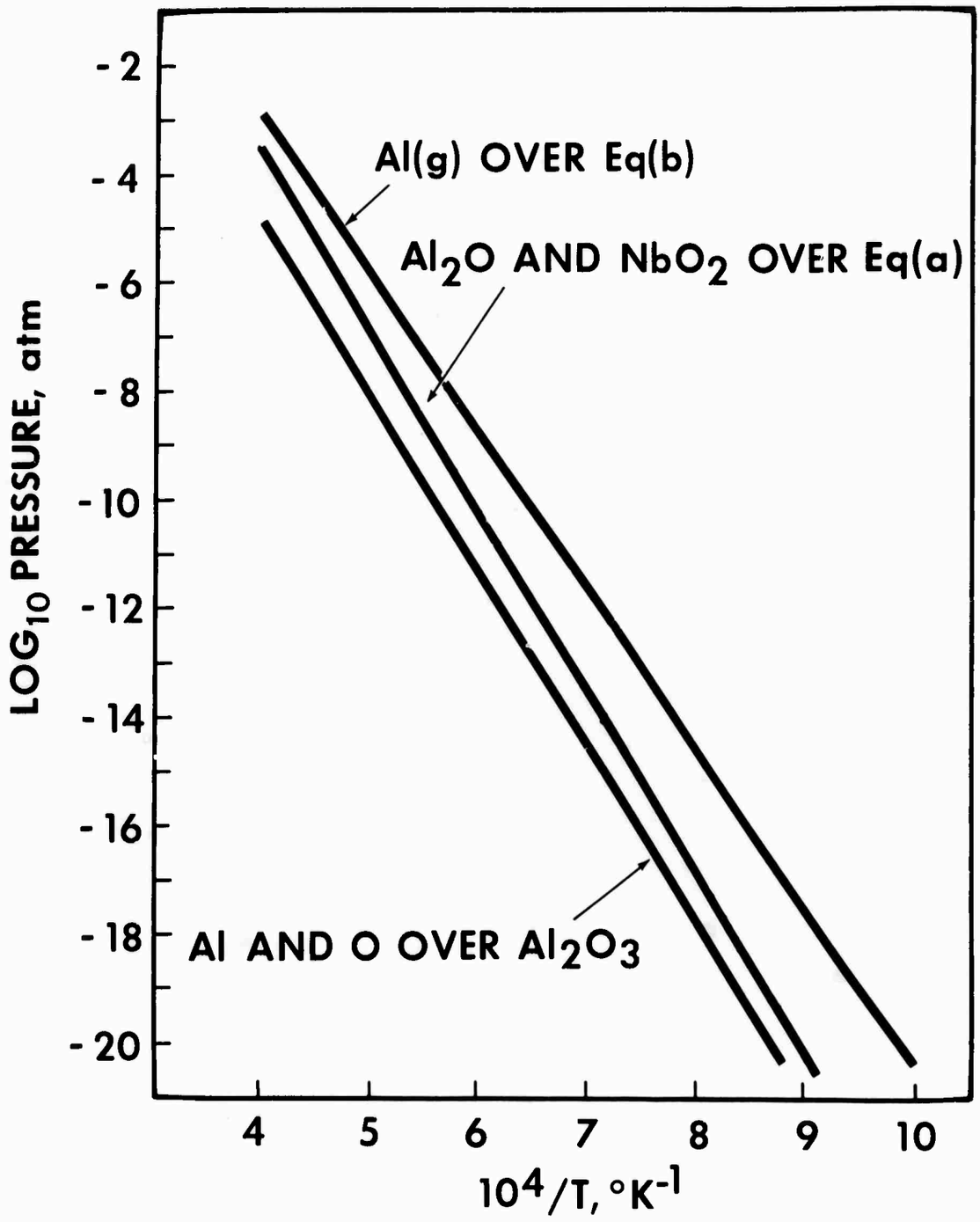

FIGURE 28. CALCULATED PRESSURES OVER Nb+Al_2O_3

partial pressures over equations (b) and (c); equation (a) is equivalent to (c) when (c) is limited by oxvgen over niobium + oxide as calculated in Figure 27. The temperature dependence of weight loss predicted by equations (b) and (c) is identical in slope and similar in magnitude to the observed weight loss (Figure 26). The predicted weight losses are twice those observed at all temperatures studied.

The observed weight loss rates (Figure 26) are about two orders of magnitude greater than evaporation loss of alumina under neutral conditions.[33] The observed reactions between alumina and niobium are driven by the stable volatile products Al(g) or $Al_2O(g)$. Calculations using available thermodynamic data[32, 34] have shown that refractory oxides other than alumina can be used successfully with niobium because their gaseous species are less stable. Table 8 gives calculated gaseous reaction product pressures over some likely reactions between niobium and some oxides at 2000°K. Beryllia weight loss will be about doubled by the presence of niobium and niobium oxide(s) will be formed if these two contact. Yttria (and other stable oxides of low vapor pressure metals) will not react appreciably with niobium. Table 8 shows that the most favored yttria-niobium reaction yields $NbO_2(g)$ and YO(g); the total pressure of reaction products at 2000°K is about an order of magnitude less than the oxide decomposition pressure. This

TABLE 8.

Predicted Reactions Between Niobium and Some Oxides at 2000°K

Oxide	Oxide Decomposition Pressure (Atmosphere)	Reaction	Total Pressure of Reaction Products
Al_2O_3	$10^{-7.8}$	$Al_2O_3 + 3Nb = 2Al(g) + 3NbO(s)$	$10^{-6.2}$
		$Al_2O_3 + 2Nb + 1/2\ O_2 =$ $NbO(s) + Al_2O(g) + NbO_2(g)$	$10^{-6.6}$
BeO	$10^{-7.4}$	$BeO + Nb = Be(g) + NbO(s)$	$10^{-7.6}$
Y_2O_3	$10^{-8.8}$	$Y_2O_3 + 3Nb = 2Y(g) + 3NbO(s)$	$10^{-12.1}$
		$Y_2O_3 + Nb = 2YO(g) + NbO(s)$	$10^{-10.6}$
		$2Y_2O_3 + Nb = NbO_2(g) + 4YO(g)$	$10^{-9.6}$
ThO_2	$10^{-9.1}$	$ThO_2 + Nb = ThO(g) + NbO(s)$	$10^{-16.2}$
		$ThO_2 + 1/2\ Nb =$ $ThO(g) + 1/2\ NbO_2(g)$	$10^{-10.4}$

predicted compatibility and the similarity between thermal expansivities of niobium and Y_2O_3 make them likely candidate materials for high temperature metal-ceramic joins.

Conclusions

The equilibrium reaction between alumina and niobium preceeds principally as $Al_2O_3 + 3Nb = 2Al(g) + 3NbO(s)$; a secondary reaction of almost equal importance under neutral conditions is $Al_2O_3 + Nb + 1/2\,O_2 = Al_2O(g) + NbO_2(g) + NbO(s)$. The secondary reaction can dominate under oxidizing conditions. Weight loss due to the gaseous reaction products of the two reactions is about one hundred times the weight loss due to evaporation of alumina under neutral conditions. Y_2O_3 and some other oxides can be used at high temperatures with niobium with no significant reaction.

Acknowledgments

Grateful appreciation is extended to N.R. Mullison who conducted the mass spectrometric and thermogravimetric experimentation. D.M. Rooney and J.E. Lewis performed the metallographic and X-Ray analyses, respectively. Appreciation is also extended to C. Chavis who built the electron bombardment power supply based on prints supplied by R. Rau (Argonne National Laboratory), and to L.F.

Epstein, A.I. Kaznoff, and A.W. Searcy (University of California at Berkeley) for their helpful review of the manuscript.

REFERENCES

1. Grossman, L. N., Kaznoff, A. I., and Stephas, P., "Structural and Emitter Materials for Nuclear Thermionic Converters," in Metallurgy of Semiconductor Materials, Ed., J. B. Schroeder, Vol. 15, Interscience, 1962.

2. Grossman, L. N., Ekvall, R. A., and Hill, H. W., "Uranium Oxide Fuel for Nuclear Thermionic Converters" International Conference on Thermionic Electrical Power Generation, London, September 1965.

3. Research and Development Program of Thermionic Conversion of Heat Electricity, Final Technical Summary Report, Vol, II, GEST-2035, June 30, 1964.

4. Martin, A. E., and Edwards, K. E., J. Phys. Chem. 69, 1788 (1965).

5. Kaznoff, A. I., Sanderson, M. J. and VanHoomissen, J. E., "Interaction and Diffusion in the UO_2-Mo System," ANS Trans 7, 1, 100 (1964).

6. Kaznoff, A. I., Sanderson, M. J., and VanHoomissen, J. E., "Interaction and Diffusion in the UO_2-Mo System," ANS Trans. 8 2, 32 (1956).

7. Sanderson, M. J., Grossman, L. N. Hill, H. W., and Kaznoff, A. I., "Compatibility of Nuclear Fuel and Thermionic Emitter Materials," Thermionic Conversion Specialist Conference, Gatlinburg, Tenn., October 1963.

8. VanHoomissen, J. E. and Kaznoff, A. I., "Compatibility of UO_2-Tungsten Thermionic Emitters in Ex-Reactor Converter Environment," ANS Trans. 7, 2, 376 (1964).

9. J. S. Anderson, et. al., Nature 185, 916 (1960).

10. J. Rothwell, Nucl. Mtl. 6, 229 (1962).

11. L. N. Grossman, R. A. Ekvall, and H. W. Hill, "Uranium Oxide Fuel for Nuclear Thermionic Converters," General Electric Vallecitos Atomic Laboratory Report GEST-2053. Paper presented at International Conference on Thermionic Electrical Power Generation, September 1965.

12. A. E. Martin and R. K. Edwards, J. of Phys. Chem. 69, May 1965.

13. J. Crank, "The Mathematics of Diffusion," Oxford at Clarendon Press, (1956) P. 66.

14. "Technical Summary Report of Research and Development Program of Thermionic Conversion of Heat to Electricity," Semi-Annual Report GEST-2046, December 31, 1964, P. 13.

15. W. N. Platte, "Joining of Molybdenum," WADC Technical Report 54-17. Part 3. March 1956, P. 50.

16. G. W. Brock, "Strain Aging Effects in Arc-Cast Molybdenum," Trans AIME No. 5, October 1961, P. 1055.

17. E. G. King, W. W. Weller, and A. V. Christensen, "Thermodynamics of Some Oxides of Molybdenum and Tungsten," Bureau of Mines RI-5664, 1960.

18. P. G. Shewman, "Diffusion in Solids," McGraw-Hill Book Co., New York, 1963, P. 2.

19. S. Dushman and J. M. Lafferty, "Scientific Foundations of Vacuum Techniques," John Wiley & Sons, Chap. 10, 2nd edition, 1962.

20. "A Metallurgical Study of Mo," Eleventh Quarterly Report, BMI, March 1, 1952.

21. A. H. Cottrell, Phil. Mag. 44, 829 (1953).

22. J. Stringer and P. S. Rudman, First Quarterly Report, Battelle Memorial Institute, November 3, 1964.

23. R. W. Powers and M. V. Doyle, J. of Applied Physics, 30, January-June 1959, P. 514.

24. A. J. Jacobs, "Diffusion of Oxygen in Tungsten and Some Other Transition Metals," Nature 200, No. 4913, 1963, P. 1310.

25. P. G. Shewman, op. cit., p. 164.

26. Cowan, R. E. and S. D. Stoddard, "Ceramic Materials for Nuclear Thermionic Converters," presented at 65th Annual Meeting of the American Ceramic Society, Pittsburgh, Pa. (May 1, 1965).

27. Ackerman, R. J. and R. J. Thron, Progress in Ceramic Science, Vol. 1, J. E. Burke, ed., Pergamon Press, p. 73.

28. Knudsen, M., Ann. Physik 29, 179 (1909).

29. Seybolt, A. U., Trans. AIME 200, 774-776 (1954).

30. Inouye, H., "The Oxidation of Columbium at Low Oxygen Pressures," in Columbium Metallurgy, Interscience, N. Y. (1960).

31. Clausing, P., Ann. Physik 29, 961 (1932).

32. JANAF Thermochemical Tables; Dow Chemical Company, Midland, Michigan,

33. Drowart, J., G. DeMaria, R. P. Burns, and M. G. Inghram, J. Chem. Phys. 32, 1366-1372 (1960).

34. Thermodynamics of Nuclear Materials, International Atomic Energy Agency, Vienna (1962), p. 417-440 and 450.

35. L. N. Grossman, "Niobium-Al_2O_3 Reactions Yielding Condensed and Volatile Products," J. Chem. Phys. 44, 4127-4131 (1966).

APPENDICES

APPENDIX A

Method for Determining the Diffusivity of Oxygen in Mo from the Average concentration of Rods

It was mentioned previously[1] that Fick's second law diffusion equation can be solved for an infinitely long solid cylinder if two boundary conditions are known and if the diffusivity is not a function of concentration.[2] The solution of the diffusion equation for the above conditions is:

$$[C(r) - C_i]/[C_o - C_i] = 1 - 2/a \sum_{n=1}^{\infty} e^{-D\alpha_n^2 t} J_o(r, \alpha_n)/J_1(a, \alpha_n) \qquad (A-1)$$

where C(r) is the concentration of oxygen at a radius r after time t; C_i is the initial uniform concentration of oxygen in the cylinder; C_o is the concentration of oxygen at the surface of the rod; a is the rod radius; D is the diffusivity; t is the time; r is the radial distance from the center of the rod; J_o and J_1 are Bissel functions of order zero and one, respectively; and α_n is the root of $J_o(\alpha_n, a) = 0$. If the solution for the cylinder is written in terms of two dimensionless parameters, Dt/a^2 and r/a, a family of curves is obtained when $[C(r) - C_i]/[C_o - C_i)$ is plotted versus r/a (one curve for each value of Dt/a^2). The particular family of curves which one obtains depends on the rate of supply of oxygen to the external cylinder surface which is characterized by a transfer coefficient β. This coefficient is analyogous to the surface coefficient, HC, applied to heat flow problems.[3] The remainder of the discussion in this appendix applies equally well to a

family of curves for any given β. No two curves of a family cross; thus, the area under each curve is uniquely determined by Dt/a^2. The area under each curve of the family of curves $r\,[C(r) - C_i]/[C_o - C_i]$ vs r/a is also uniquely determined by Dt/a^2.

The area, A, under each curve is given by,

$$A = \int_{r/a=o}^{r/a=1} r \frac{(C(r) - C_i)}{(C_o - C_i)} \; d\left(\frac{r}{a}\right). \qquad (A\text{-}2)$$

which simplifies to,

$$A = \frac{1}{a(C_o - C_i)} \left[\int_{r/a=o}^{r/a=1} C(r)\, r dr - C_i \int_{r/a=o}^{r/a=1} r dr \right] \qquad (A\text{-}3)$$

Multiplying the first integral of equation (A-3) by $2\pi\ell/2\pi\ell^2$ (where ℓ is the cylindrical rod length) and integrating the second integral, we obtain

$$A = \frac{1}{a(C_o - C_i)} \left[\frac{1}{2\pi\ell} \int_{r/a=o}^{r/a=1} C(r)\, \ell 2\pi r dr - C_i \frac{a^2}{2} \right] \qquad (A\text{-}4)$$

A cylindrical element of volume of thickness, dr, at constant radius, r, is given by $2\pi\ell r dr$. C(r) is the oxyben concentration throughout this volume element; thus $C(r)\, 2\pi\ell r dr$ is the number of oxygen atoms in the volume element. Thus, $\int_{r/a=1}^{r/a=o} C(r)\, \ell 2\pi r dr$ equals the total number of oxygen atoms, N, in the whole cylinder of radius, a, [if C(r) has units of oxygen atomx/unit volume]. Substituting N into equation (A-4) we find,

$$A = \frac{1}{a(C_o - C_i)} \left[\frac{1}{2\pi\ell} N - C_i \frac{a^2}{2} \right] \qquad (A-5)$$

Consider now only the first term inside the brackets of equation (A-5). Multiplying the top and bottom of this term by the total volume, V, we obtain $V/2\pi\ell \cdot N/V$; but N/V is the average concentration of oxygen, C_{av}, in the rod. Substituting $V/2\pi\ell \cdot C_{av}$ into equation (A-4) and remembering $V = \pi a^2 \ell$ we obtain,

$$A = \frac{1}{a(C_o - C_i)} \left[\frac{\pi a^2 \ell}{2\pi\ell} C_{av} - \frac{C_i a^2}{2} \right] \qquad (A-6)$$

which simplifies to

$$A = \frac{a(C_{av} - C_i)}{2(C_o - C_i)} \qquad (A-7)$$

Thus, the area under a given curve corresponding to a given value of Dt/a^2 is related to the average concentration of oxygen in the rod by equation (A-7) and C(r) need not be evaluated.

The most useful form of equation (A-7) for the present work is:

$$C_{av} = \frac{2(C_o - C_i) A}{a} + C_i \qquad (A-8)$$

Appendix A Bibliography

1. "Technical Summary Report of Research and Development Program of Thermionic Conversion of Heat to Electricity," Semi-Annual Report GEST-2046,

2. J. Crank, "The Mathematics of Diffusion," Oxford at the Clarendon Press, 1956, p. 66.

3. J. B. Austin, "The Flow of Heat in Metals," ASM Book, 1942, p. 120.

APPENDIX B

Estimation of Equilibrium Solubility of Oxygen in Molybdenum as a Function of Temperature

To calculate values for diffusivities of oxygen in molybdenum from Fick's first law at temperatures in the range 1500 to 1800°C, the oxygen concentration gradients in the molybdenum had to be known. From the present experimental studies with molybdenum capsules, the oxygen concentration on the outside capsule surface at 1800°C was found to be 5 ppm and the concentration on the inside capsule surface was found to be 39 ppm at 1500°C. Since this data was insufficient for calculating ΔC at any of the temperatures of interest, several assumptions were made to obtain approximate values of ΔC. First, the outside concentration of 5 ppm found at 1800°C was used for capsules at all temperatures. Second, the concentration at the inside surface of the capsule at each temperature was estimated from the experimental value obtained at 1500°C and oxygen solubility data reported by Few and Manning.[1] They reported a solubility limit for oxygen in molybdenum as a function of temperature as shown by the solid portion of curve A of Figure B-1. The dashed portion of the curve, A, is an extrapolation of their data to 1800°C. They exposed samples to oxygen pressures well in excess of equilibrium pressures for the formation of molybdenum oxygen (solid) and determined solubility limits by the microscopic metal presence or absence of oxide in their samples. This procedure and analytical technique could easily lead to high values of the solubility limit. The oxygen pressure of the

Curve A Few and Manning
Curve B Interpolation between A and C
Curve C Extrapolation of present data

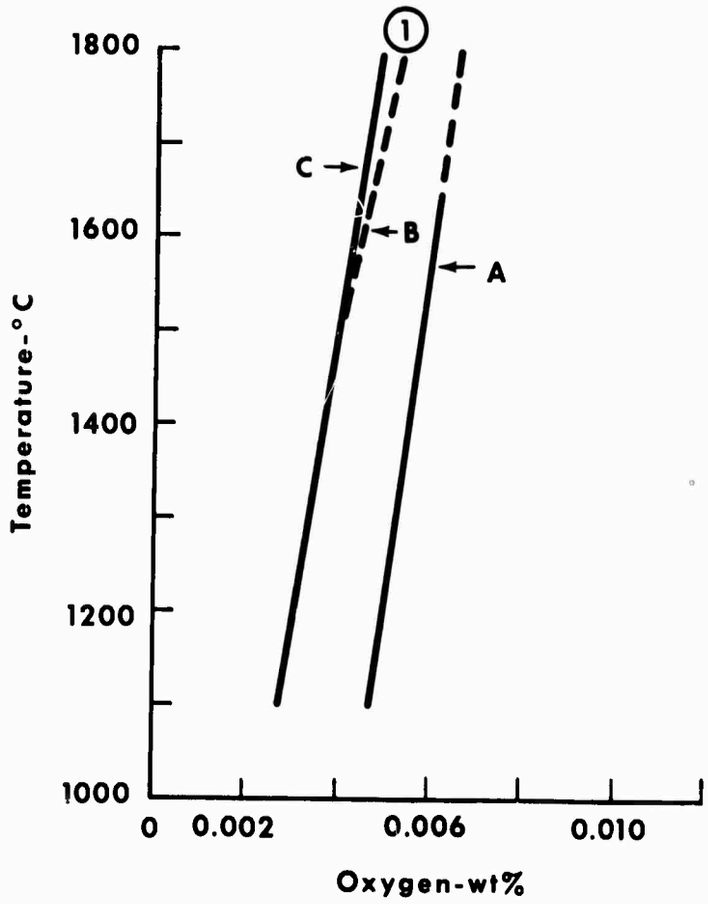

FIGURE B-1. SOLUBILITY LIMIT OF OXYGEN IN MOLYBDENUM

present experiments was very close to the equilibrium value. Because of this, the value of 39 ppm at 1500°C is believed to be more accurate than Few and Manning's data. To estimate the concentrations at the inside capsule surface for temperatures higher than 1500°C, the slope of Curve A is assumed to be correct and a curve C parallel to curve A and passing through 39 ppm at 1800°C was constructed. In addition to the temperature dependence shown by curve C we would expect (from Henry's Law) a contribution to the solubility at each temperature above 1500°C from the increased equilibrium pressure relative to the pressures used by Few and Manning. The pressures used by Few and Manning differed from the equilibrium pressures used in the present investigation, as shown in Table B-I. The pressure ratio (Table B-I) decreased with increasing temperature showing that the equilibrium pressure at 1800°C was approximately one order of magnitude or 25% closer to the pressure used by Few and Manning than the equilibrium pressure at 1500°C. The pressure contribution to the solubility of oxygen at 1800°C was therefore estimated to be approximately 1/4 of the concentration difference between curves A and C or point (1) of Figure B-1. The solid solubility of oxygen at intermediate temperature was estimated by constructing the dashed straight line B from 39 ppm at 1500°C to 53 ppm (point (1)) at 1800°C. The resulting solubility limits were 48, 44, and 34 ppm at 1700, 1600, and 1400°C, respectively.

In preliminary experiments, Rudman[3] found a solubility of oxygen in molybdenum of 45 ± 5 ppm at 1800°C. This tends to support the method of estimation used above rather than the data of Few and Manning.

TABLE B-I

Oxygen Test Pressures

Temperature (°C)	Pressure (microns) (1) Few & Manning	(2) Present Study**	Pressure Ratio (1) : (2)
1500	2.5×10^{2}	1.2×10^{-2}	2.08×10^{4}
1600	7.4×10^{2}	7.5×10^{-2}	1×10^{4}
1700	1.9×10^{3} *	3.8×10^{-1}	5×10^{3}
1800	4.1×10^{3} *	1.9	2.2×10^{3}

*Extrapolated from Few and Manning's work.

**King and Weller[2] data were used.

Appendix B Bibliography

1. W. E. Few and G. K. Manning, "Solubility of Carbon and Oxygen in Molybdenum," J. of Metals, March 1952, p. 271.

2. E. G. King, W. W. Weller, and A. V. Christensen, "Thermodynamics of Some Oxides of Molybdenum and Tungsten," Bureau of Mines, RI-5664, 1960.

3. P. S. Rudman, Fourth Quarterly Progress Report, Battelle Memorial Institute, June 1, 1965.